PERTURBATION ANALYSIS IN DIELECTRIC LOADED RECTANGULAR WAVEGUIDES

A Thesis

Presented to

The Faculty of Graduate Studies and Research

The University of Manitoba

In Partial Fulfillment

of the Requirements for the Degree

Master of Science in Electrical Engineering

---

by

Satish Chander Kashyap

September 1968

ABSTRACT

Wave propagation in rectangular waveguides loaded with dielectric slabs is investigated using perturbation theory. Richter, Diament and Schlesinger's Perturbation analysis, which is a modification, extension and generalization of time dependent quantum mechanical perturbation theory is extended to deal with more general cases. In particular, results are obtained for one or several dielectric slabs with faces parallel to, and at arbitrary distances away from the waveguide walls. It is shown, contrary to Richter's conclusion, that the theory leads to reasonable agreement with experiment and available rigorous solutions even when the magnitude of a certain perturbation parameter is allowed to exceed unity. This parameter depends upon the type of the perturbation, its size and the relative change in medium parameters.

ACKNOWLEDGEMENTS

The author expresses his sincere appreciation to Professor M.A.K. Hamid who suggested the problem and took an active interest in the work throughout.

Sincere thanks are due to many faculty members and colleagues for their comments and discussions. The author expresses his appreciation to Miss S. Yamaguchi for the excellent typing of the manuscript.

The financial assistance of the National Research Council, under Grant A-3326, and the Defence Research Board, under Grant 6801-37 is also acknowledged.

TO MY PARENTS

WITH DEEP GRATITUDE AND AFFECTION

TABLE OF CONTENTS

LIST OF FIGURES

CHAPTER I

INTRODUCTION

There has been considerable effort in recent years to interpret the behaviour of dielectric loaded waveguides from the calculation of their associated propagation function [1 -5] . Such waveguides have been used in the past as phase shifters [6] , slow wave structures [2,4] and recently as models for ferrite devices, in particular non-reciprocal phase shifters [5] and isolators [7] . Furthermore they have been found to offer much greater bandwidth and power handling capacity than unloaded waveguides [2].

An exact formulation for isotropic dielectrics is easily accomplished using transverse resonance techniques [8,9] . These techniques normally yield a transcendental equation, which must then be solved numerically for the propagation constant. Some variational and graphical solutions for E-plane slabs have also been developed [3,10]. These methods are either restricted to small values of the dielectric constant or special slab geometries or sometimes to single or double slabs only. However these restrictions have to be removed in many of the devices mentioned above.

Recourse is had to perturbation theories whenever exact solutions are not available or are unwieldy. Moreover in many cases the approximate perturbation analysis may yield sufficiently accurate results to diminish the merit of an exact solution.

The aim of the present thesis is to calculate the propagation constant and related parameters for a number of geometries involving dielectric loaded rectangular waveguides. Richter's Perturbation theory

[11-14] is extended to deal with one or more slabs oriented in the E or H plane and with varying geometrical configurations. These results are compared with experiment or available rigorous solutions leading to a good agreement in most cases.

An interesting result of this investigation is that, contrary to Richter's theory[14] good results have been obtained even when the magnitude of a certain perturbation parameter is larger than unity. This parameter is directly related to the type of perturbation, its size and the relative change in medium parameters as will be shown in Chapter II. The deviation from other theories or experiment is found to increase when the propagation constant is perturbed from a real to an imaginary value or when the dielectric constant is very high.

The theory is applied in Chapter III to a finite slab of mixed dielectrics with particular application to grain samples infested with insects. The results of these calculations are also in favourable agreement with experiment.

Finally, the advantage of the perturbation theory is that it provides a simple and systematic approach for the calculation of approximate values for the propagation constant and related parameters.

CHAPTER II

DIELECTRIC SLAB PERTURBATION

2.1 INTRODUCTION

The word "perturb" means to disturb, change or vary slightly. Perturbation methods are particularly applicable whenever the problem under consideration closely resembles one which is exactly solvable. Usually two problems are involved, the unperturbed problem for which the solution is known and the perturbed problem which is slightly different from the unperturbed one. If both the unperturbed and the perturbed systems are discribed by an eigenvalue equation, "a time independent or static" theory may be used. If the perturbed equation is however is not separable into eigenvalue equations, so that a set of characteristic modes does not exist, "time dependent perturbation theory" [15] is used.

A recent contribution to "time independent or static" theory [16-20]is a method proposed by Richter [11-14] which is basically an extension of time dependent perturbations in quantum mechanics, with axial co-ordinate replacing time. However in the electromagnetic case this method takes into account the phase progression of the perturbed wave which is usually ignored in quantum theory.

2.2 GENERAL PROBLEM

The perturbation analysis presented here can be applied to all boundary value problems which can be represented in the form

$$([A_o] + [A])[\psi] = \delta[\psi]/\delta z \tag{2.2.1}$$

where the unknown wave function ψ may be an n-vector function of the axial co-ordinate z and of any number of other co-ordinates. Matrices

$[A]$ and $[A_o]$ are linear differential n x n matrix operators not containing derivatives with respect to z. It is assumed that matrix $[A_o]$ is independent of the z co-ordinate, but may be any function of the transverse co-ordinates. Its perturbation matrix $[A]$ however, may be a function of all co-ordinates, but is restricted only in the sense that the set of mode functions ψ_p must remain complete and orthogonal for the perturbed region. The unperturbed eigenvalue equation is

$$A_o\psi_o = \frac{\delta\psi_o}{\delta z} = -j\beta\psi_o \tag{2.2.2}$$

where ψ_o is the mode function in the absence of the perturbation and is assumed to have a set of mode functions

$$\psi = \psi_p e^{-j\beta_p z}$$

Here the n-vector functions ψ_p are independent of the axial co-ordinate and, for appropriate boundary conditions, are complete and orthogonal in the xy plane. Depending on the nature of the problem they may be a discrete set, where p is an integer, or may span a continuous spectrum, in which case p is not necessarily an integer. Note that, for simplicity, only a single mode $\psi_o = \psi_1$ is assumed to be present in the absence of the perturbation. If in some class of problems, it is necessary to have more than one mode propogating in the absence of the perturbation, the assumed linearity of equation(2.2.1) allows appropriate superposition of the perturbed solutions.

2.3 E-PLANE DIELECTRIC SLAB PERTURBATION

Consider an empty rectangular waveguide of cross-sectional dimensions a and b. For this case the unperturbed wave equation is given by

$$\begin{bmatrix} o & j\omega\mu_o \\ -\frac{1}{j\omega\mu_o}\frac{\delta^2}{\delta x^2} + j\omega\varepsilon_o & o \end{bmatrix}\begin{bmatrix} E_y \\ H_x \end{bmatrix} + \begin{bmatrix} o & o \\ j\omega\varepsilon_o(\varepsilon-1) & o \end{bmatrix}\begin{bmatrix} E_y \\ H_x \end{bmatrix} = \frac{\delta}{\delta z}\begin{bmatrix} E_y \\ H_x \end{bmatrix} \tag{2.3.1}$$

as shown in appendix A2.1. This equation is of the same form as (2.2.2) and its solutions are given by the well-known modal expansion

$$\begin{bmatrix} E_y \\ \\ H_x \end{bmatrix} = \begin{bmatrix} -\omega\mu_c/\beta_n \\ \\ 1 \end{bmatrix} \sin(n\pi x/a)\ e^{-j\beta_n z} = \psi_n e^{-j\beta_n z} \tag{2.3.2}$$

where

$$\beta_n = \pm\sqrt{k^2\varepsilon - n^2\pi^2/a^2} \quad \text{for } n>c,\ \beta_n = -\beta_{-n} \tag{2.3.3}$$

and

$$k^2 = \omega^2\mu_o\varepsilon_o \tag{2.3.4}$$

If the waveguide is now perturbed by a perturbation of relative dielectric constant $\varepsilon(x,z)$ as shown in figure (2.3.1a) then the perturbation matrix [A] is given by

$$[A] = \begin{bmatrix} o & o \\ \\ 1 & o \end{bmatrix} j\omega\varepsilon_o(\varepsilon(z) - 1)h(x-x_1)h(x_2-x) \tag{2.3.5}$$

where h is the Heaviside unit step function and ψ_o in the present case is taken to be

$$\psi_o = \psi_1 = \begin{bmatrix} \dfrac{-\omega\mu_o}{\beta_1} \\ 1 \end{bmatrix} \sin(\pi x/a) e^{-jk_z z} \tag{2.3.6}$$

2.3.1 FORM OF PERTURBED FIELDS

The solution of equation (2.2.1) is assumed to be of the form

$$\psi = \psi_o e^{-j[\beta_o z + f_o(z)]} + \Phi \tag{2.3.7}$$

Here the total field has been expressed as a sum of the incident mode ψ_o, altered by a nonlinear phase progression $f_o'(z)$, and a scattered field

$$\Phi = \sum_{p\neq c} u_p(z)\ e^{-j\beta_p(z)}\psi_p \tag{2.3.8}$$

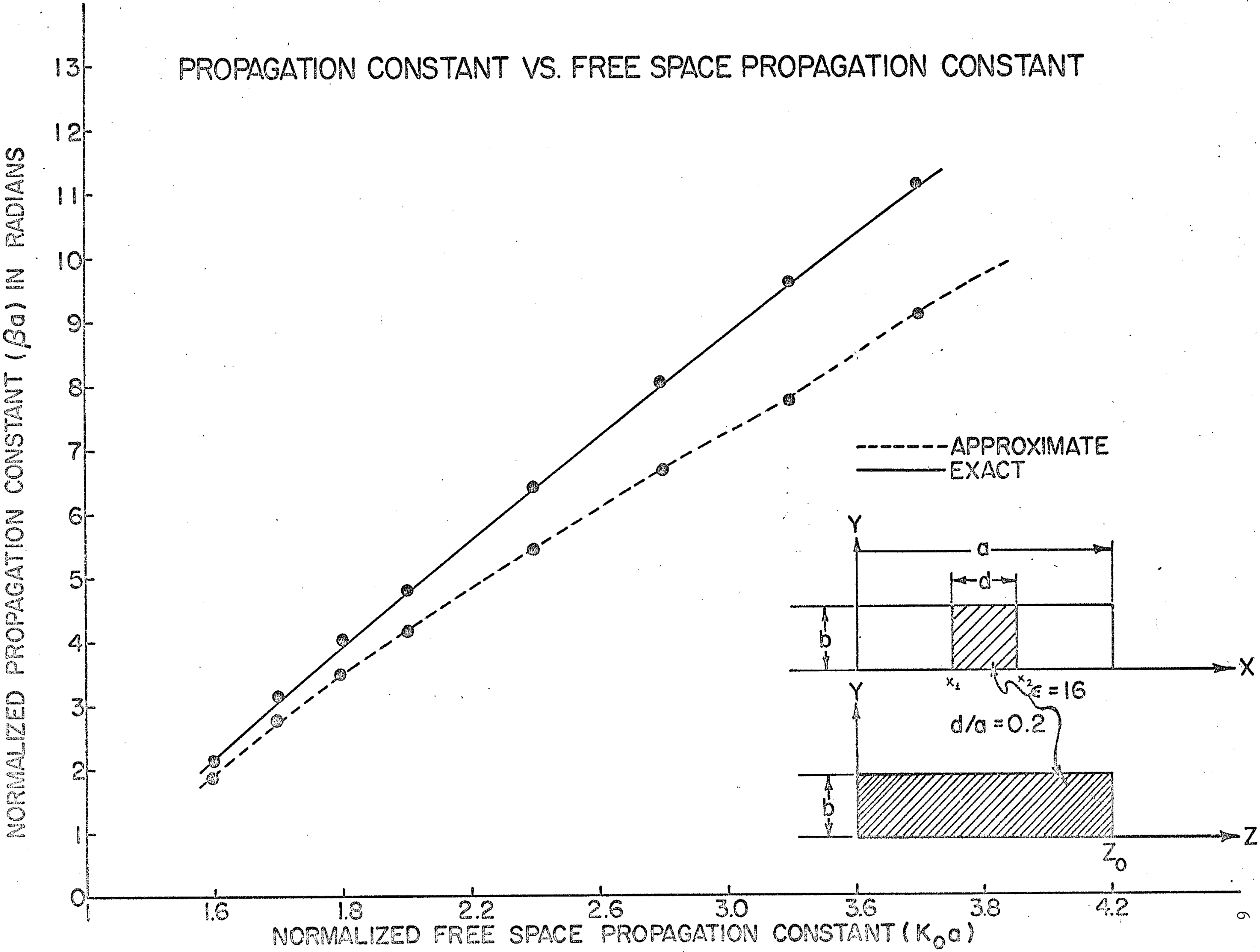
PROPAGATION CONSTANT VS. FREE SPACE PROPAGATION CONSTANT
NORMALIZED PROPAGATION CONSTANT (βa) IN RADIANS
NORMALIZED FREE SPACE PROPAGATION CONSTANT ($K_o a$)
APPROXIMATE
EXACT
Y
a
d
b
X
x_1
x_2
$\epsilon = 16$
$d/a = 0.2$
Z
Z_o
0
1
2
3
4
5
6
7
8
9
10
11
12
13
1.6
1.8
2.2
2.6
3.0
3.6
3.8
4.2

Fig. 2.3.1a

Except for the incident mode, Φ consists of a complete set of all transverse modes ψ_p. u_p are the corresponding mode coefficients. The function $f_o(z)$, which is the correction to the phase progression $\beta_o z$ of the unperturbed mode, may be a complex function in order to account for both amplitude and phase correction to the incident mode ($\psi_o = \psi_1$). Assuming that the phase of the incident mode in the absence of the perturbation is simply $\beta_o z$, we see that $f_o^{(o)} = o$ and $u_p^{(o)} = o$, where the superscript denotes the order of perturbation. Note that for the technique to be valid, the function should be expandable as a sum of functions ψ_p, which in turn should be orthogonal to ψ_o for all z. The function ψ may also be expanded as follows

$$\psi = \sum_p r_p(z)\psi_p \tag{2.3.9a}$$

or

$$\psi = \sum_p s_p(z)e^{-j\beta_p z}\psi_p \tag{2.3.9b}$$

Both of these forms lead to difficulties. First, since the complex function r_p (or s_p) is expanded in order of perturbation, with $r_p^{(o)}$ (or $s_p^{(o)}$) as the first term, it is difficult to retrieve information on the correction to the phase progression f_p, of a given mode from either r_p or s_p. In addition, if the axial extent of the perturbation is large and the average correction to the phase progression per unit length is non zero, this correction will appear to each order of perturbation as a secular term. This means that the coefficient of each mode would, to each order of perturbation, increase without bound as a function of the axial co-ordinate if the perturbation were extended over a wider axial range.

The form for ψ used in (2.3.7) is a compromise. Secular terms are avoided in the mode of interest by introducing the complex exponent $f_o(z)$. However, the fields scattered by the perturbation, as given in (2.3.8), have been expressed in a simpler form without explicitly expressing their phase progression. This is expedient because one is usually interested in the phase progression correction to the incident mode which is given by the real part of f_o. This perturbation theory in general would be valid only in those regions of perturbing structure where the scattered fields remain small compared to the incident field. However the phase progression correction f_o will not be required to be small and in fact it may grow large with z.

2.3.3 PERTURBATION EQUATIONS

Substitution of the expressions for the perturbed fields in (2.3.7) and (2.3.8) into the perturbation equation (2.2.1) yields

$$([A]+j\,df_o/dz)\psi_o e^{-j(\beta_o z+f_o)}=\sum_{p\neq o}(du_p/dz-u_p[A])\psi_p e^{-j\beta_p z} \tag{2.3.10}$$

This exact equation may now be separated into individual equations for each mode by taking scalar products with suitable functions adjoint to each mode. The scalar product of (2.3.10) with ψ_o' (where the prime notation denotes the adjoint) and ψ_q' for $q\neq o$ yields

$$\left[\frac{j\,df_o}{dz}+\frac{\langle\psi_o'|A|\psi_o\rangle}{\langle\psi_o'|\psi_o\rangle}\right]e^{-j(\beta_o z+f_o)}=-\sum_{p\neq o}u_p e^{-j\beta_p z}\frac{\langle\psi_o'|A|\psi_p\rangle}{\langle\psi_o'|\psi_o\rangle} \tag{2.3.11}$$

and

$$\frac{\langle\psi_q'|A|\psi_o\rangle}{\langle\psi_q'|\psi_q\rangle}e^{-j(\beta_o z+f_o)}=\frac{du_q}{dz}e^{-j\beta_q z}-\sum_{p\neq o}u_p e^{-j\beta_p z}\frac{\langle\psi_q'|A|\psi_p\rangle}{\langle\psi_q'|\psi_q\rangle} \tag{2.3.12}$$

respectively.

The scalar products are given by

$$\langle\psi_p'|\psi_n\rangle = \int_o^a [-1 \quad \omega\mu_o/\beta_p] \begin{bmatrix} -\omega\mu_o/\beta_n \\ 1 \end{bmatrix} \sin(p\pi x/a)\sin(n\pi x/a)\,dx \tag{2.3.13}$$

and

$$\langle\psi_p'|A|\psi_n\rangle = \int_o^a [-1 \quad \omega\mu_o/\beta_p] \begin{bmatrix} o & o \\ 1 & o \end{bmatrix} \begin{bmatrix} -\omega\mu_o/\beta_n \\ 1 \end{bmatrix} \sin(p\pi x/a)\sin(n\pi x/a)g(x,z)\,dx \tag{2.3.14}$$

where

$$g(x,z) = j\omega\varepsilon_o(\varepsilon-1) \tag{2.3.15}$$

for the present example. To separate these equations into various orders of perturbation, f_o and u_p are now expanded in the usual perturbation series

$$f = f_o^{(1)} + f_o^{(2)} + f_o^{(3)} \ldots\ldots \tag{2.3.16}$$

$$u_p = u_p^{(1)} + u_p^{(2)} + u_p^{(3)} \ldots\ldots \tag{2.3.19}$$

where each succeeding term represents a higher order of accuracy. Substitution of (2.3.16) and (2.3.17) into (2.3.11) and (2.3.12) together with the separation of the resulting equations for various orders of perturbation yieldsthe following expressions for f_o and u_p

$$\frac{df_o^{(1)}}{dz} = j\frac{\langle\psi_o'|A|\psi_o\rangle}{\langle\psi_o'|\psi_o\rangle} \tag{2.3.18}$$

$$\frac{df_o^{(i)}}{dz} = -\sum_{k=2}^{i-1} \frac{df_o^{(k)}}{dz}\,\phi^{(i-k)} + \frac{j\,\langle\psi_o'|A|\Phi^{(i-1)}\rangle e^{j\beta_o z}}{\langle\psi_o'|\psi_o\rangle}, \qquad i=2,3,4,\ldots \tag{2.3.19}$$

where

$$\phi = e^{-jf_o} = 1 + \phi^{(1)} + \phi^{(2)} + \ldots \qquad (2.3.20)$$

$$\phi^i = \sum_{p \neq o} u_p^{(i)} e^{-j\beta_p z} \psi_p \qquad (2.3.21)$$

$$\frac{du_p^{(1)}}{dz} = \frac{\langle \psi_p' | A | \psi_o \rangle}{\langle \psi_p | \psi_p \rangle} e^{-j(\beta_1 - \beta_p)z} \qquad (2.3.22)$$

$$\frac{du_p^{(i)}}{dz} = \frac{\langle \psi_p' | A | \phi^{(i-1)} \rangle}{\langle \psi_p' | \psi_p \rangle} e^{j\beta_p z} + \frac{\langle \psi_p' | A | \psi_o \rangle}{\langle \psi_p' | \psi_p \rangle} \phi^{(i-1)} e^{-j(\beta_1 - \beta_p)z}, \quad i=2,3,4,\ldots \qquad (2.3.23)$$

2.3.3. ILLUSTRATIVE EXAMPLE: E-PLANE SLAB (appendix A2.2)

The expressions for f_o and u_p in this case are given by

$$f_o^{(1)} = \frac{k^2 \chi}{\beta_1} G_{11} z \qquad (2.3.24)$$

$$u_p^{(1)} = \frac{k^2 G_{p1} \chi}{\beta_1(\beta_1 - \beta_p)} e^{-j(\beta_1 - \beta_p)z} \qquad (2.3.25)$$

$$f_o^{(2)} = \sum_p \frac{k^4 \chi^2 G_{p1}^2 z}{\beta_1 \beta_p (\beta_1 - \beta_p)} \qquad (2.3.26)$$

$$u_p^{(2)} = \frac{k^4 \chi^2 G_{11}}{\beta_1(\beta_1 - \beta_p)} e^{-j(\beta_1 - \beta_p)z} \left[\frac{G_{pp}}{\beta_p(\beta_1 - \beta_p)} - \frac{G_{11}}{\beta_1} z - \frac{G_{11}}{\beta_1(\beta_1 - \beta_p)} \right] \qquad (2.3.27)$$

$$f_o^{(3)} = \sum_p \frac{k^6\, \chi G_{p1}^2 z}{\beta_1\beta_p(\beta_1-\beta_p)^2}\left[\frac{G_{pp}}{\beta_p} - \frac{G_{11}}{\beta_1}\right] \tag{2.3.28}$$

$$f = f_o^{(1)} + f_o^{(2)} + f_o^{(3)} + \ldots.$$

and

$$= \frac{k^2\chi G_{11} z}{\beta_1} + \sum_p [\frac{k^4\chi^2 G_{p1}^2 z}{\beta_1\beta_p(\beta_1-\beta_p)}][1 + \frac{k^2\chi G_{pp}}{\beta_p(\beta_1-\beta_p)} - \frac{k^2\chi G_{11}}{\beta_1(\beta_1-\beta_p)} + \ldots], \; p \neq 1$$

where the summation over the integer p is equivalent to summation over forward and backward traveling modes. If for the dominant backward mode, i.e. $p = -1$, the forms containing β_{-1} are grouped separately, the new expression for f is given by

$$f = [\frac{k^2\chi G_{11} z}{\beta_1} - \frac{k^4\chi^2 G_{11}^2 z}{2\,\beta_1^3} + \frac{k^6\chi^3 G_{11}^3 z}{2\,\beta_1^5} + \ldots] + f' \tag{2.3.30}$$

where

$$f' = \sum_{p>1} \frac{2k^4\chi^2 G_{p1}^2 z}{\beta_1(\beta_1^2-\beta_p^2)}[1 + \frac{k^2\chi G_{pp}(\beta_1^2+\beta_p^2)}{\beta_p^2(\beta_1^2-\beta_p^2)} - \frac{2k^2\; G_{11}}{\beta_1^2-\beta_p^2} + \ldots] \tag{2.3.31}$$

Here the phase constants for the backward modes have been expressed in terms of the phase constants for the forward modes using the relation $\beta_p = -\beta_{-p}$. The resulting expression for the propagation constant is given by

$$k_z = f + \beta_1 z \tag{2.3.32}$$

or

$$k_z / \beta_1 z = [1 + \frac{2k^2\chi G_{11}}{\beta_1^2}]^{\frac{1}{2}} + f'/\beta_1 \tag{2.3.33}$$

where the terms in the square brackets in (2.3.31) have been summed as a binomial series, and

$$G_{pq} = \frac{1}{a}\int_{x_1}^{x_2} \sin(p\pi x/a)\,\sin(q\pi x/a)\,dx\ , \quad \chi = \varepsilon - 1 \tag{2.3.34}$$

Figures (2.3.1a–f) show the results for the E-plane dielectric slab perturbations of various geometries where the computations are based on (2.3.31) to (2.3.33). The cut off wavelength λ_c, in figure (2.3.1e) is approximately given by

$$\frac{2k_c^{\,2}\chi G_{11}}{\beta_1^{\,2}} = -1, \quad k_c = \frac{2\pi}{\lambda_c} \tag{2.3.35}$$

where k_c equals k when k_z in (2.3.33) is equal to zero.

The propagation constant for the eleven slab case shown in Figure (2.3.2) is obtained using the same expression except that χ is now a function of x and G_{pq} is given by

$$G_{pq} = \frac{1}{a}\int_{x_o+d_i}^{x_o+d_{i+1}} \chi_i\,\sin(p\pi x/a)\,\sin(q\pi x/a)\,dx\ , \quad i=1,2,.. \tag{2.3.36}$$

instead of (2.3.34). The integrals in (2.3.36) are straightforward and lead to the result

$$G_{pq} = \frac{1}{2\pi}\sum_i \chi_i\left[\frac{\sin\{(\pi x/a)(p-q)\}}{p-q} - \frac{\sin\{(\pi x/a)(p+q)\}}{p+q}\right]_{x+d_i}^{x+d_{i+1}} \tag{2.3.37}$$

2.4. APPLICATION TO THE DIELECTRIC WAVEGUIDE PHASE SHIFTER

Consider an E-plane dielectric slab perturbation of finite axial length ℓ which is the case of a waveguide dielectric slab phase shifter. The first order expressions for this case have been given in [1]. They are reproduced here along with the expressions for higher order terms.

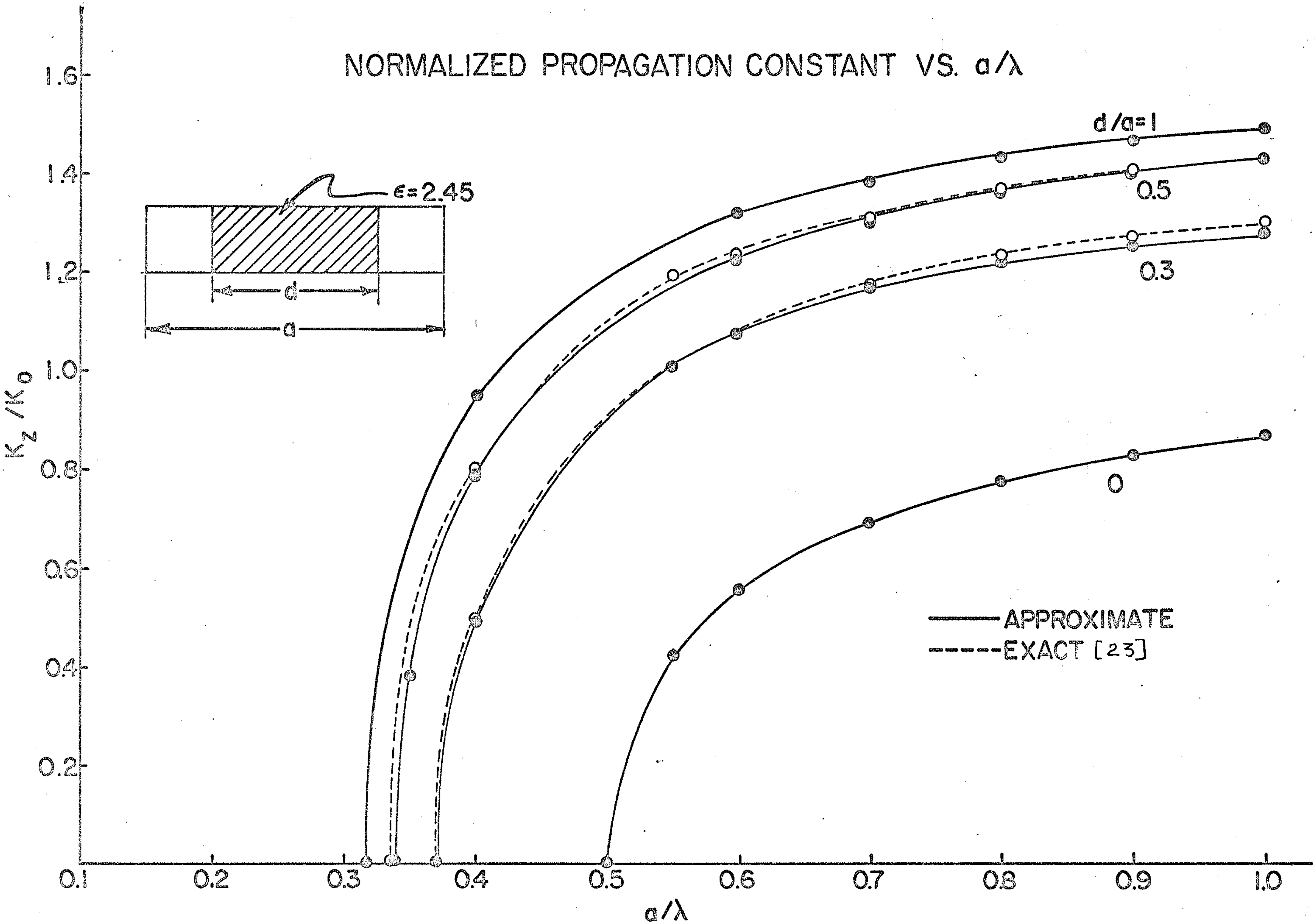
NORMALIZED PROPAGATION CONSTANT VS. a/λ
ε=2.45
d
a
d/a=1
0.5
0.3
0
APPROXIMATE
EXACT [23]
K_z/K_0
a/λ
1.6
1.4
1.2
1.0
0.8
0.6
0.4
0.2
0.1
0.2
0.3
0.4
0.5
0.6
0.7
0.8
0.9
1.0
Fig. 2.3.1b

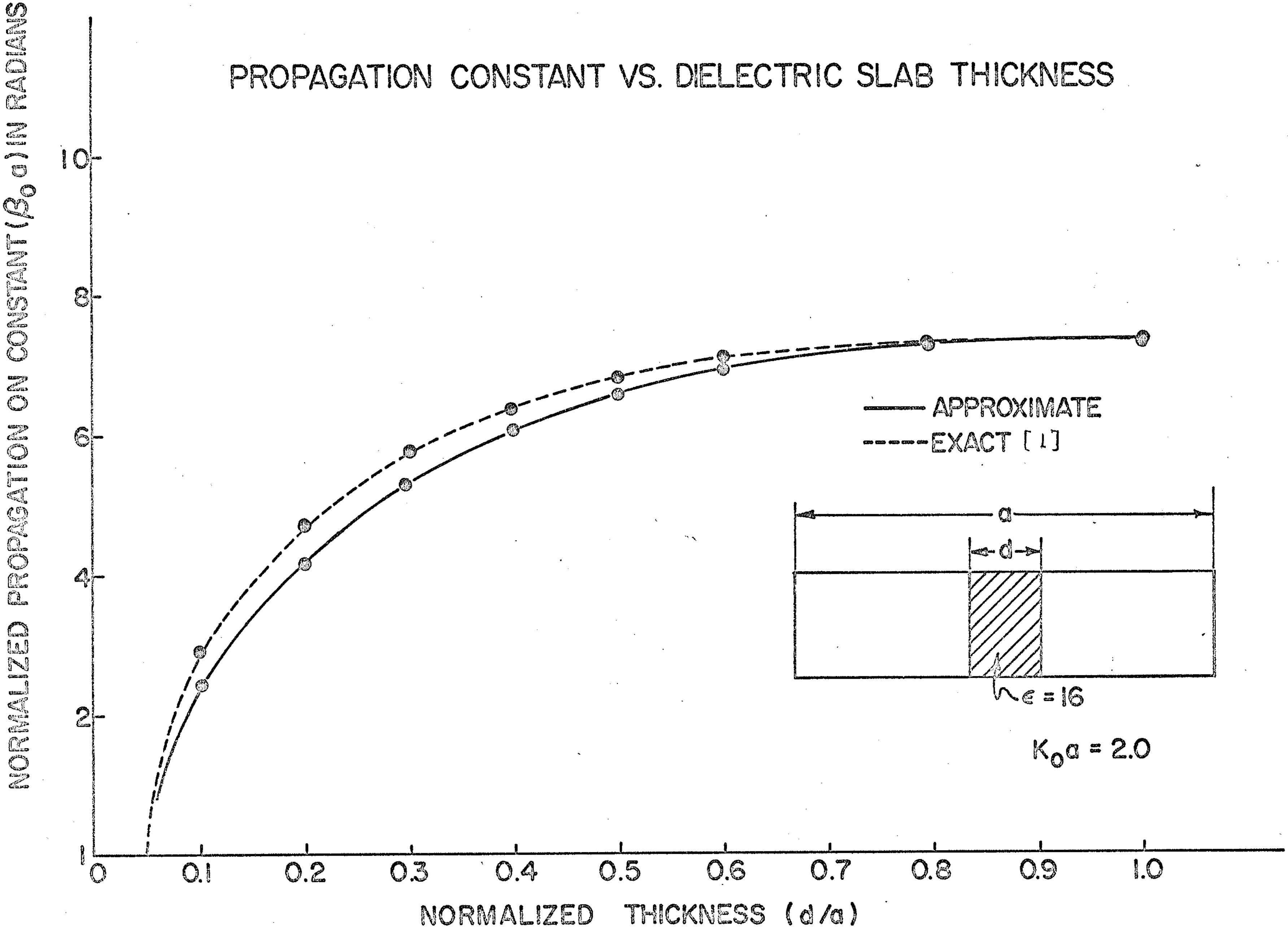
PROPAGATION CONSTANT VS. DIELECTRIC SLAB THICKNESS
NORMALIZED PROPAGATION ON CONSTANT ($\beta_0 a$) IN RADIANS
10
8
6
4
2
1
0
0.1
0.2
0.3
0.4
0.5
0.6
0.7
0.8
0.9
1.0
NORMALIZED THICKNESS (d/a)
APPROXIMATE
EXACT [1]
a
d
$\epsilon = 16$
$K_0 a = 2.0$

Fig. 2.3.1c

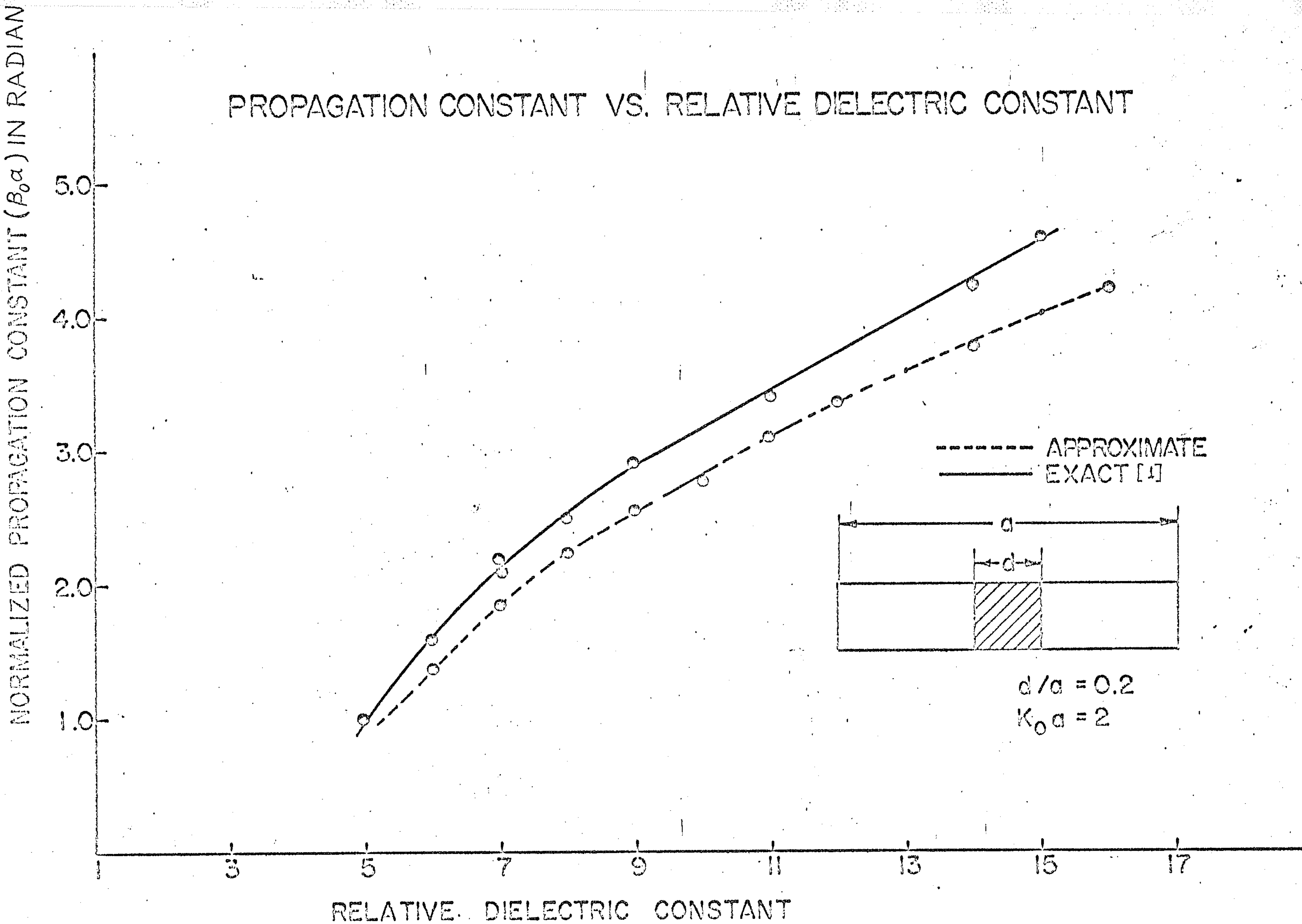
PROPAGATION CONSTANT VS. RELATIVE DIELECTRIC CONSTANT
NORMALIZED PROPAGATION CONSTANT ($\beta_o a$) IN RADIAN
5.0
4.0
3.0
2.0
1.0
1
3
5
7
9
11
13
15
17
RELATIVE DIELECTRIC CONSTANT
APPROXIMATE
EXACT [1]
a
d
d / a = 0.2
$K_o a = 2$

Fig. 2.3.1d

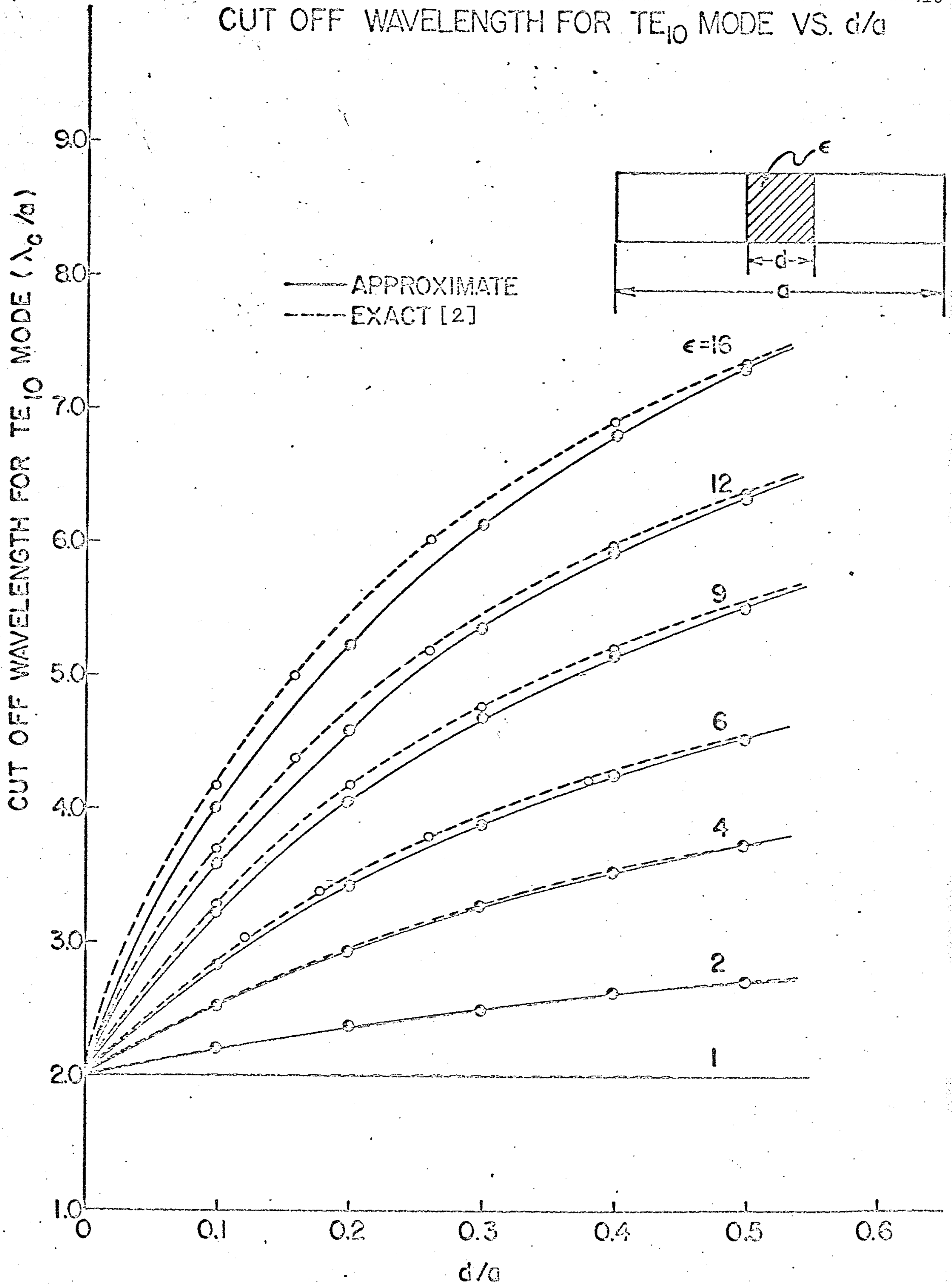
CUT OFF WAVELENGTH FOR TE_{10} MODE VS. d/a
CUT OFF WAVELENGTH FOR TE_{10} MODE (λ_c/a)
APPROXIMATE
EXACT [2]
ϵ
d
a
ϵ=16
12
9
6
4
2
1
1.0
2.0
3.0
4.0
5.0
6.0
7.0
8.0
9.0
0
0.1
0.2
0.3
0.4
0.5
0.6
d/a

Fig. 2.3.1e

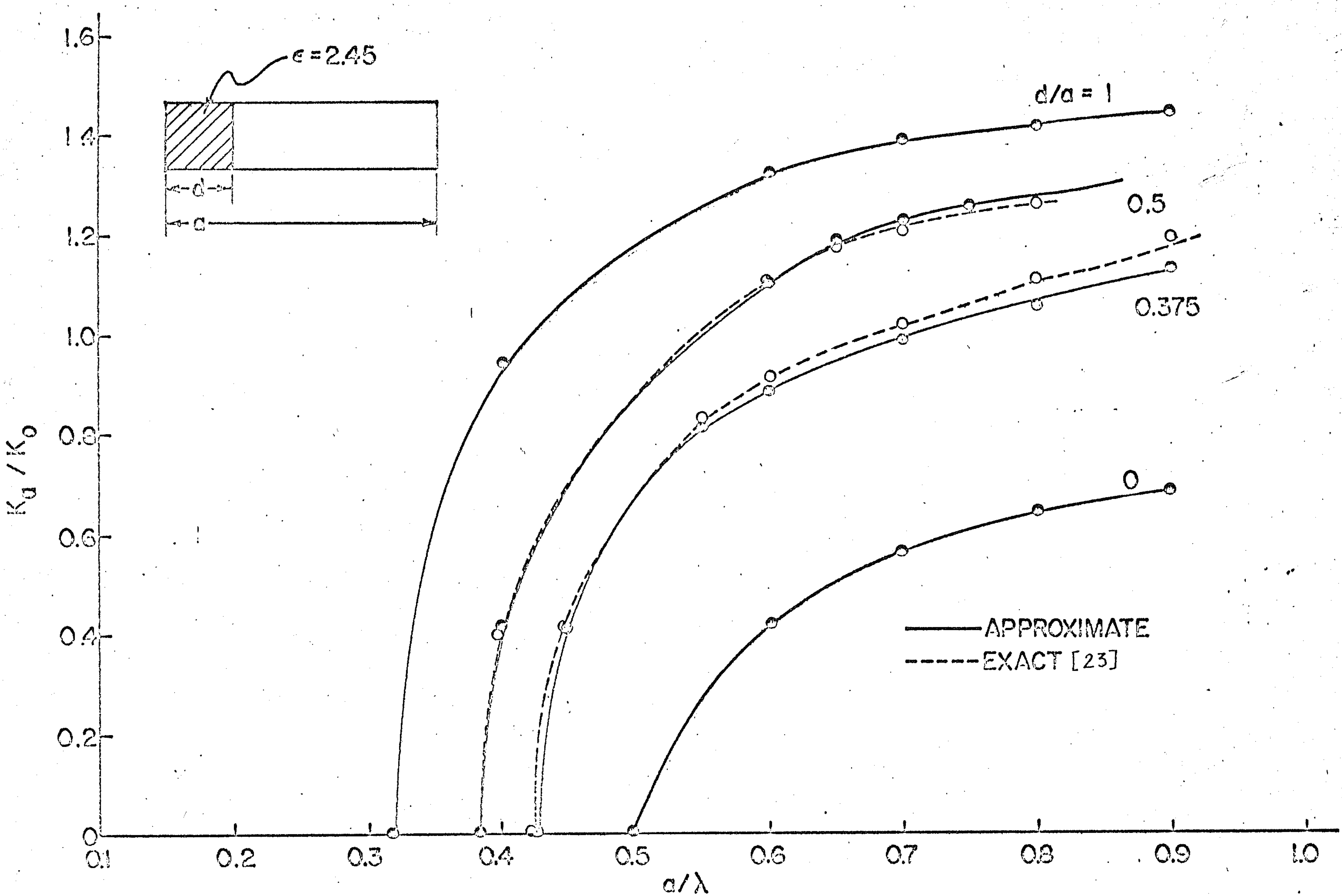

NORMALIZED PROPAGATION CONSTANT VS. a/λ Fig. 2.3.1f

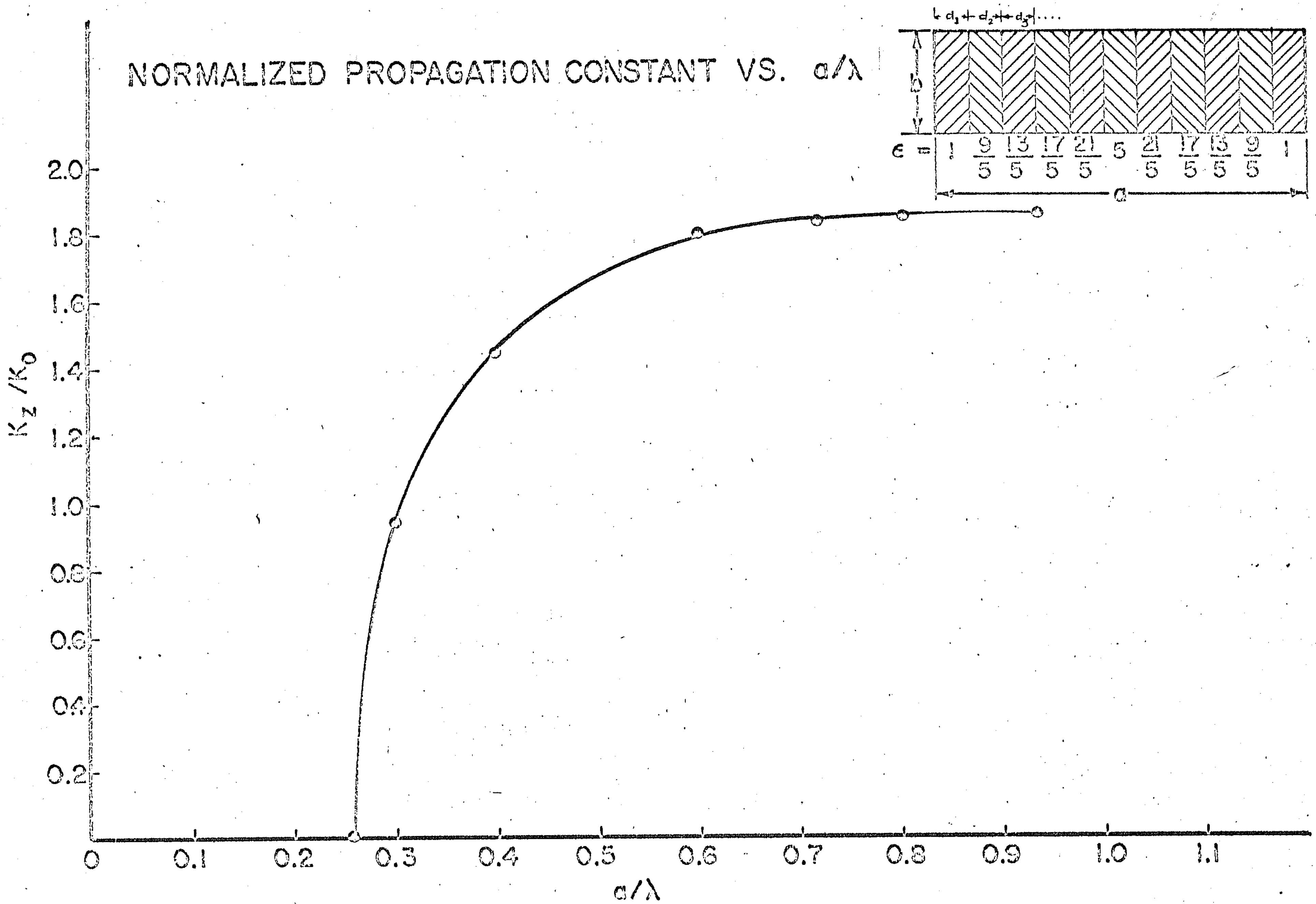
NORMALIZED PROPAGATION CONSTANT VS. a/λ
d1 d2 d3 ...
b
ε = 1 9/5 13/5 17/5 21/5 5 21/5 17/5 13/5 9/5 1
a
Kz /Ko
2.0
1.8
1.6
1.4
1.2
1.0
0.8
0.6
0.4
0.2
0 0.1 0.2 0.3 0.4 0.5 0.6 0.7 0.8 0.9 1.0 1.1
a/λ

Fig. 2.3.2

$$f_o^{(1)}(z) = \frac{k^2\chi}{\beta_1} G_{11}(x_1,x_2)z \qquad o \leq z \leq \ell \qquad (2.4.1)$$

$$u_p^{(1)} = \frac{k^2\chi}{\beta_1} G_{p1}(x_1,x_2)h(z)\frac{e^{-j(\beta_1-\beta_p)\min(z,\ell)}-1}{\beta_1-\beta_p} \qquad p>1 \qquad (2.4.2)$$

$$= \frac{k^2\chi}{\beta_1} G_{p1}(x_1,x_2)h(\ell-z)\ \frac{e^{-j(\beta_1-\beta_p)zh(z)}-e^{-j(\beta_1-\beta_p)\ell}}{(\beta_1-\beta_p)} \qquad p<o \qquad (2.4.3)$$

where min(z,ℓ) equals zero or ℓ, whichever is greater, and h is the Heaviside unit step function.

$$f_o^{(2)} = \sum_p \frac{k^4\chi^2G_{p1}^2}{\beta_1\beta_p(\beta_1-\beta_p)} \left[z + \frac{2j}{\beta_1-\beta_p} \cos\{(\beta_1-\beta_p)z/2\}\ e^{-j(\beta_1-\beta_p)(\ell-z/2)} \right],\ p<0 \qquad (2.4.4)$$

$$= \sum_p \frac{k^4\chi^2G_{p1}^2}{\beta_1\beta_p(\beta_1-\beta_p)} \left[z + \frac{j}{\beta_1-\beta_p} \{ e^{j(\beta_1-\beta_p)z} - 1 \} \right],\ p>1 \qquad (2.4.5)$$

$$u_p^{(2)} = \frac{k^4\chi^2G_{p1}}{\beta_1(\beta_1-\beta_p)} \left[\frac{G_{pp}}{\beta_p(\beta_1-\beta_p)} \{ e^{-j(\beta_1-\beta_p)z} - e^{-j(\beta_1-\beta_p)\ell} \} + \right.$$

$$\frac{j\,G_{pp}}{\beta_p} e^{-j(\beta_1-\beta_p)\ell}(z-\ell) - \frac{j\,G_{11}}{\beta_1}(ze^{-j(\beta_1-\beta_p)z} - \ell e^{-j(\beta_1-\beta_p)\ell}) -$$

$$\left. \frac{G_{11}}{\beta_1(\beta_1-\beta_p)} (e^{-j(\beta_1-\beta_p)z} - e^{-j(\beta_1-\beta_p)\ell}) \right],\ p<0 \qquad (2.4.6)$$

$$= \frac{k^4\chi^2G_{p1}}{\beta_1(\beta_1-\beta_p)} \left[\frac{G_{pp}}{\beta_p(\beta_1-\beta_p)} (e^{-j(\beta_1-\beta_p)z} - 1) + \frac{jG_{pp}z}{\beta_p} \right.$$

$$\left. - \frac{jG_{11}z}{\beta_1} e^{-j(\beta_1-\beta_p)z} - \frac{G_{11}}{\beta_1(\beta_1-\beta_p)} (e^{-j(\beta_1-\beta_p)z} - 1) \right],\ p>1 \qquad (2.4.7)$$

For the integrations required to arrive at these results, the lower limit is chosen in such a way that the constants of integration vanish, using the fact that u_p vanishes for $z < o$ in the case of positively traveling modes ($p > o$) and for $z > \ell$ in the case of negatively traveling modes ($p < o$).

The final result for the phase shift, normalized with respect to the electrical length of the slab, is the real part of $f/\beta_1\ell$ as stated in [4]. For $\beta_1\ell >> 1$ this quantity is obtained by setting $z = \ell$ and neglecting small terms in the expansion for f leading to the same result as may be obtained directly from (2.3.22) and (2.3.23). This is due to the fact that for $\beta_1\ell >> 1$ the leading terms in the expansions for $f_o^{(2)}$, $f_o^{(3)}$ .... are much greater than the rest of the terms. If only these leading terms are taken into account the expression obtained for f_o is the same as that obtained from (2.3.22) and (2.3.23). This approximation amounts to neglecting the reflections from the second interphase of the perturbation and is thereby valid only for long slabs.

2.4.2 PHYSICAL INTERPRETATION

It is difficult to account physically for all the terms in the general case (2.4.1 to 2.4.7). To achieve a better insight, a simplification is now made. The perturbation is allowed to be uniform over the entire width of the waveguide such that

$$G_{pq}(x_1,x_2) = G_{pq}(o,a) = \pm\tfrac{1}{2} \text{ for } p = \pm q \qquad (2.4.8)$$

$$= o \text{ for } p \neq q$$

The summation over the modes now reduces to one term only for the reflected dominant mode u_{-1}. Upon collecting terms to various orders, the nonlinear phase progression $f_o(z)$ is found to be

$$f_o(z) = \{z(\frac{k^2\chi}{2\beta_1} - \frac{k^4\chi^2}{8\beta_1^3} + \frac{k^6\chi^3}{16\beta_1^5} + \ldots)$$

$$+ e^{-2j\beta_1\ell}\ (j\ [\frac{k^4\chi^2}{16\beta_1{}^4} - \frac{k^6\chi^3}{16\beta_1{}^6} + \ldots\ldots] + \frac{k^6\chi^3}{16\beta_1{}^5} + \ldots\ldots)$$

$$-e^{-2j\beta_1(\ell-z)}(j[\frac{k^4\chi^2}{16\beta_1{}^4} - \frac{k^6\chi^3}{16\beta_1{}^6} + \ldots.] + (\ell-z)\frac{k^6\chi^3}{16\beta_1{}^5} + \ldots\ldots) + \ldots\} \quad o<z<\ell \tag{2.4.9}$$

$f_o(z)$ vanishes for $z<o$, and for $z>\ell$, it is constant at the value obtained by putting $z=\ell$ in (2.4.9). Equation (2.4.9) will now be interpreted in detail and, for convenience, is rewritten in the form

$$f_o(z) = Bz + C - e^{-2j\beta_1(\ell-z)}\ D + \ldots \tag{2.4.10}$$

The first term, Bz, clearly represents the correction to the phase progression of the incident mode in a medium with a dielectric constant $\varepsilon\varepsilon_o$ instead of ε_o. The actual value of B from exact analysis is given by

$$B = \beta_1' - \beta_1$$

where

$$\beta_1' = \sqrt{k^2\varepsilon - \pi^2/a^2}$$

$$= \sqrt{k^2\varepsilon_o - \pi^2/a^2 + k^2\varepsilon_o(\varepsilon-1)}$$

$$\sqrt{\beta_1{}^2 + k^2\chi} \tag{2.4.11}$$

Hence, for this example, the perturbation formulation has the effect of expanding the square root for β_1' in the binomial expansion

$$\beta_1' = \beta_1 + \frac{k^2\chi}{2\beta_1} - \frac{k^4\chi^2}{8\beta_1{}^3} + \frac{k^6\ \chi^3}{16\beta_1{}^5} - \ldots \tag{2.4.12}$$

Note that convergence may be expected for this term of f_o only when the binomial expansion converges, which corresponds to $|k^2\chi/\beta_1{}^2|<1$. The remaining terms of $f_o(z)$ in (2.4.10) may be explained by two physical effects. First, there is a change in the amplitude of the forward traveling mode due to the multiple reflections. Second, the actual TE_{1o} mode, obtained from an exact solution in the perturbed region, does not have the same wave impedance as the unperturbed mode. Thus the actual forward traveling mode is a linear combination of unperturbed forward and backward traveling modes as shown by the relation.

$$\begin{bmatrix} 1 \\ \dfrac{-\omega\mu_o}{\beta_1'} \end{bmatrix} \sin(\pi x/a) = \left\{ \begin{bmatrix} 1 \\ \dfrac{-\omega\mu_o}{\beta_1} \end{bmatrix} \frac{\beta_1 + \beta_1'}{2\beta_1'} + \begin{bmatrix} -1 \\ \dfrac{-\omega\mu_o}{\beta_1} \end{bmatrix} \frac{\beta_1 - \beta_1'}{2\beta_1'} \right\} \sin(\pi x/a) \qquad (2.4.13)$$

Similarly, the actual backward traveling wave is a linear superposition of both types of unperturbed waves. Thus in the expansion of $e^{-jf_o(z)}$ there should be terms with a propagation factor $e^{-2j\beta_1(\ell-z)}$, as well as terms containing $\dfrac{\beta_1 + \beta_1'}{2\beta_1'}$. These factors must also appear in the expansion for $f_o(z)$ and in fact the terms C and D in (2.4.10) represent respectively the forward and the backward traveling wave amplitudes contributed by the positively traveling unperturbed mode in the expansions (2.3.7) and (2.3.8).

2.5 EXPERIMENTAL SET UP FOR PHASE MEASUREMENT

The results obtained in Section 2.4 were compared (figure 2.5.1) with an experimental measurement of the phase shift using a standard bridge [21,22]. The experiment was set up as shown in figure (2.5.2).

Procedure

The signals from the reference and the unknown arms of the bridge are

PHASE SHIFT VS. POSITION OF A DIELECTRIC SLAB

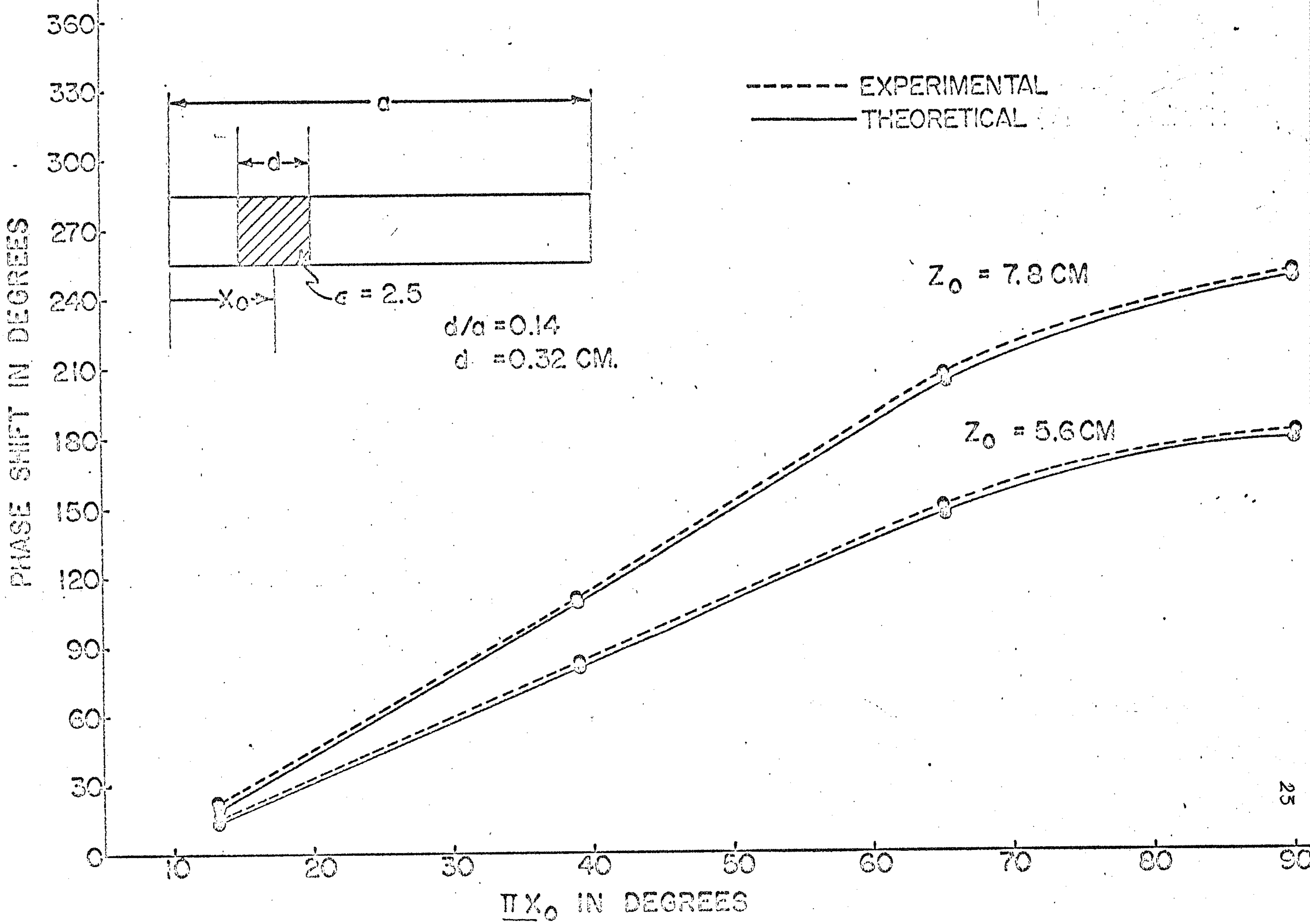

Fig. 3.5.1

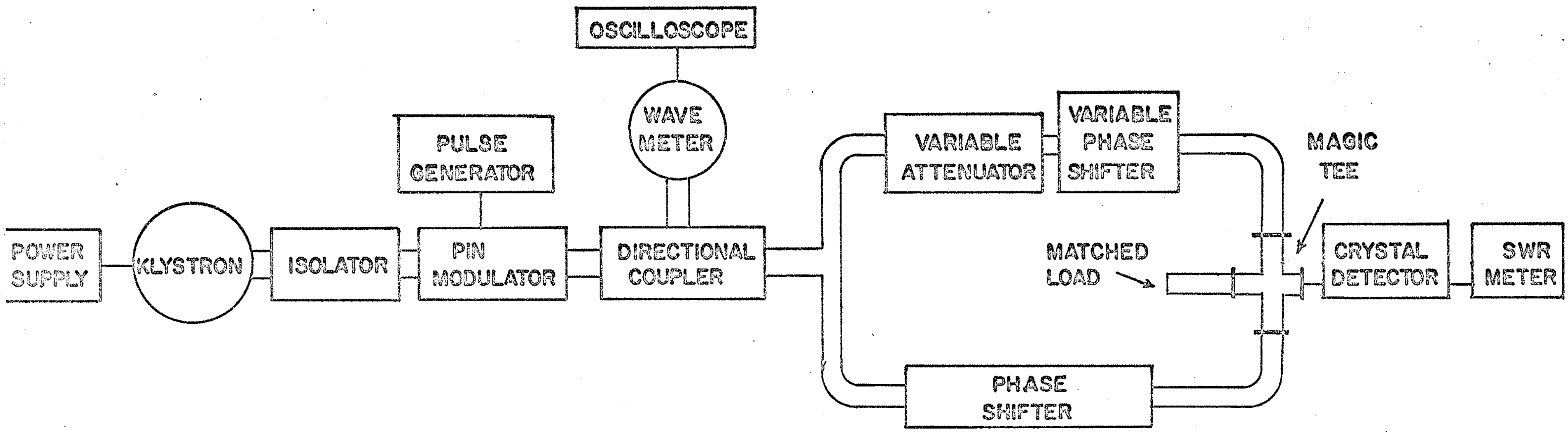

SET UP FOR PHASE MEASUREMENT

Fig. 2.5.2

fed to the two input arms of the magic tee. Any difference in the two signals is indicated by the detector in the difference arm. This difference is initially brought to a minimum by adjusting the variable attenuator and variable phase shifter in the reference arm. On the introduction of a dielectric slab in the unknown arm, the detector reading is found to change. The variable attenuator and phase shifter are adjusted to bring the detector reading to its initial value. The change in their reading gives the attenuation and phase shift introduced by the dielectric slab phase shifter. The phase shift is found to be dependent upon the position of the slab. The change is small if the dielectric slab is placed in the weakest portion of the electric field and a larger change is produced if the dielectric slab is placed in the stronger portion of the electric field. The phase shift is also a function of the dielectric material, its dimensions, and the frequency. With regard to the accuracy of the measurement we note that

1) The attenuation was found to be negligible.
2) Since the dielectric slab was moved by hand, there is some degree of uncertainty in the location of the slab.
3) Due to some leakage, it was not possible to obtain an absolute null even when the two signals were equal.

2.6 H-PLANE PERTURBATION

Consider a waveguide loaded by an H-plane perturbation of semi-infinite length as shown in figure (2.6.1). The scattered modes in such a waveguide are TM to y [8] and the wave function in a matrix form is given by

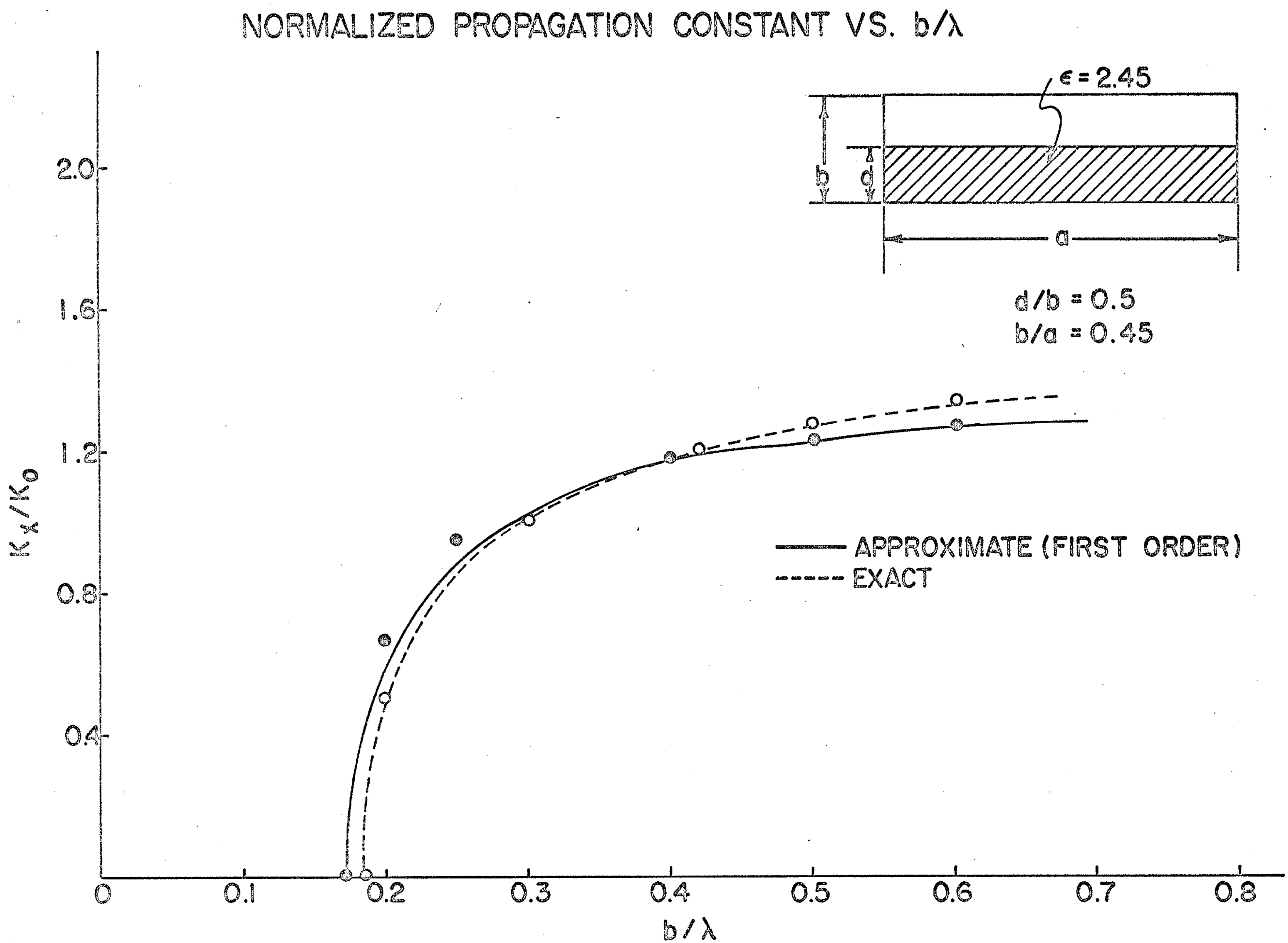
NORMALIZED PROPAGATION CONSTANT VS. b/λ
ε = 2.45
b
d
a
d/b = 0.5
b/a = 0.45
APPROXIMATE (FIRST ORDER)
EXACT
K_x/K_0
b/λ
2.0
1.6
1.2
0.8
0.4
0
0.1
0.2
0.3
0.4
0.5
0.6
0.7
0.8

Fig. 2.6.1

$$\psi_{mn} = \begin{bmatrix} E_y \\ \\ H_x \end{bmatrix} = \begin{bmatrix} \dfrac{k^2-(n\pi/b)^2}{\omega\varepsilon_o\beta_{mn}} \\ \\ 1 \end{bmatrix} \sin(m\pi x/a)\cos(n\pi y/b)e^{-jk_z z} \qquad (2.6.1)$$

where

$$\beta_{mn} = \sqrt{k^2-(m\pi/a)^2-(n\pi/b)^2} \qquad (2.6.2)$$

for a waveguide of dimensions a and b. The incident mode in this case may be chosen as TM_{10} to y which is the same as the TE_{10} mode and is given by

$$\psi_o = \psi_{10} = \begin{bmatrix} \dfrac{-\omega\mu_o}{\beta_{10}} \\ \\ 1 \end{bmatrix} \sin(\pi x/a)e^{-jk_z z} \qquad (2.6.3)$$

The matrix $[A_o]$ is given by (appendix A2.4)

$$[A_o] = \begin{bmatrix} o & \dfrac{-1}{j\omega\varepsilon_o}\dfrac{\partial^2}{\partial y^2} + j\omega\mu_o \\ \dfrac{1}{j\omega\mu_o}\dfrac{k^2}{k^2-(n\pi/b)^2}\dfrac{\partial^2}{\partial x^2} + j\omega\varepsilon_o & o \end{bmatrix} \qquad (2.6.4)$$

and its perturbation matrix [A] by

$$[\,A\,] = \begin{bmatrix} o & \dfrac{-1}{j\omega\varepsilon_o}(1/\varepsilon-1)\dfrac{\partial^2}{\partial y^2} \\ \\ -j\omega\varepsilon_o(\varepsilon-1) & o \end{bmatrix} \qquad (2.6.5)$$

Here the scalar products are given by

$$\langle \psi'_{m'n'} | \psi_{mn} \rangle = \frac{k^2-(n\pi/b)^2}{\omega\varepsilon_o\beta_{mn}} \frac{ab}{2} \quad \delta_{mm'}\delta_{nn'} \qquad (2.6.6)$$

and

$$\frac{\langle \psi'_{m'n'} | A | \psi_{mn} \rangle}{\langle \psi'_{m'n'} | \psi_{mn} \rangle} = \frac{\omega\varepsilon_o\beta_{10}}{k^2} \left[-j\frac{k^2-(n'\pi/b)^2}{\omega\varepsilon_o\beta_{m'n'}} \cdot \frac{k^2-(n\pi/b)^2}{\omega\varepsilon_o\beta_{mn}} \omega\varepsilon_o\chi + \frac{1}{j\omega\varepsilon_o} (1/\varepsilon-1)\left(\frac{n\pi}{b}\right)^2 \right] \times G_{mm'nn'} \qquad (2.6.7)$$

where

$$G_{mm'nn'} = \frac{1}{ab} \int_{o}^{b/2} \int_{o}^{a} \sin(m\pi x/a)\sin(m'\pi x/a)\cos(n\pi y/b)\cos(n'\pi y/b)dx\, dy \qquad (2.6.8)$$

Using (2.3.24) to (2.3.33) and the equations developed above, the solution, considering only the scattered mode β_{-10}, is given by

$$\frac{k_z}{\beta_{10}{}_z} = (1 + 2\, G_{1100} \frac{k^2\chi}{\beta_1^2})^{1/2} \qquad (2.6.9)$$

The results are compared with the available rigorous solution [23] as shown in figure (2.6.1).

2.7 CONVERGENCE AND LIMITATIONS OF THE METHOD

Like most other perturbation techniques, the success of this technique depends to some extent on the rate of convergence of the perturbation series.

In general a perturbation series might be said to converge if for all orders i of perturbation higher than a specific order, the ratio of the i^{th} order scattered fields $\phi^{(i)}$ at some point in space to that of $\phi^{(i-1)}$ at the same point is less than some constant (with respect to i) which is smaller than unity.

As mentioned earlier the perturbation matrix [A] should be small compared with [A_o] in some sense. The actual condition on the size required for the validity of the technique may depend upon the type of perturbation, its physical size with respect to the wavelength and the order to which one is willing and able to carry out the computations. However it is not the large physical size itself, the type of perturbation, or the large change in medium parameters, but rather the combination of all these quantities, which limits the validity of the technique. This point will be now explained more clearly. For a perturbation which completely fills the cross-section of the waveguide

$$k_z = \beta_1 \left(1+ \frac{k^2 \chi}{\beta_1^2}\right)^{\frac{1}{2}} \qquad (2.7.1)$$

The factor $k^2\chi/\beta_1^2$ in (2.7.1) is replaced by $2G_{11}k^2\chi/\beta_1^2$, for the general case, and may be referred to as the perturbation parameter. This parameter is directly related to the frequency, the medium parameters, the type and the size of the perturbation. One can use the theory for any value of this perturbation parameter if the contribution from the dominant scattered mode were sufficient to get accurate results. This is possible because these contributions have been expressed in a closed form.. However the contributions from the dominant mode are not always sufficient and higher order modes have to be considered to improve the accuracy in many cases. Since the contributions from the dominant mode have not been put in a closed form, some restrictions have to be put, if extremely accurate results are desired. Thus for extreme accuracy G_{11} or G_{pq} should be small, while χ should be small and less than $\beta_1^2/2G_{11}k^2$. The first two conditions, although they imply that the phase progression correction and the scattered modes are small to the first order, do not necessarily imply that the higher order terms are small compared to the first order terms. The third condition ensures the latter.

CHAPTER III

APPLICATION TO THE MIXED DIELECTRICS

3.1 INTRODUCTION

The results of the theory developed in Chapter II can be utilized to find the properties of a finite slab of mixed dielectrics which in this chapter are assumed to be grain and insects.

3.2 EQUIVALENT DIELECTRIC CONSTANT

The equivalent complex dielectric constant of a mixture of two lossy dielectrics is given by [24].

$$\varepsilon'/\varepsilon_H' = 1/4\{-[(1-3\xi)(\varepsilon_I'/\varepsilon_H') + 3\xi - 2] + \sqrt{[(1-3\xi)(\varepsilon_I'/\varepsilon_H') + 3\xi - 2]^2 + 8\varepsilon_I'/\varepsilon_H'}\} \qquad (3.2.1)$$

Here the subscript H denotes the host medium (grain) and I denotes the inclusions (insects). In the derivation of (3.2.1) it is assumed that the host medium is homogeneous and isotropic while the inclusions are randomly distributed spheres. ξ is the volume concentration of the insects normalized with respect to the volume of the grain. The results for $\varepsilon'/\varepsilon_H' - 1$ vs ξ are shown graphically in figure (3.2.1). Since the dielectric loss in a particular volume of the mixture is directly related to the complex part of the dielectric constant, these results can be utilized for the detection of insects in samples of infested grain.

3.3 SCATTERING COEFFICIENTS

The reflection coefficient of a slab of finite length ℓ is given by [12]

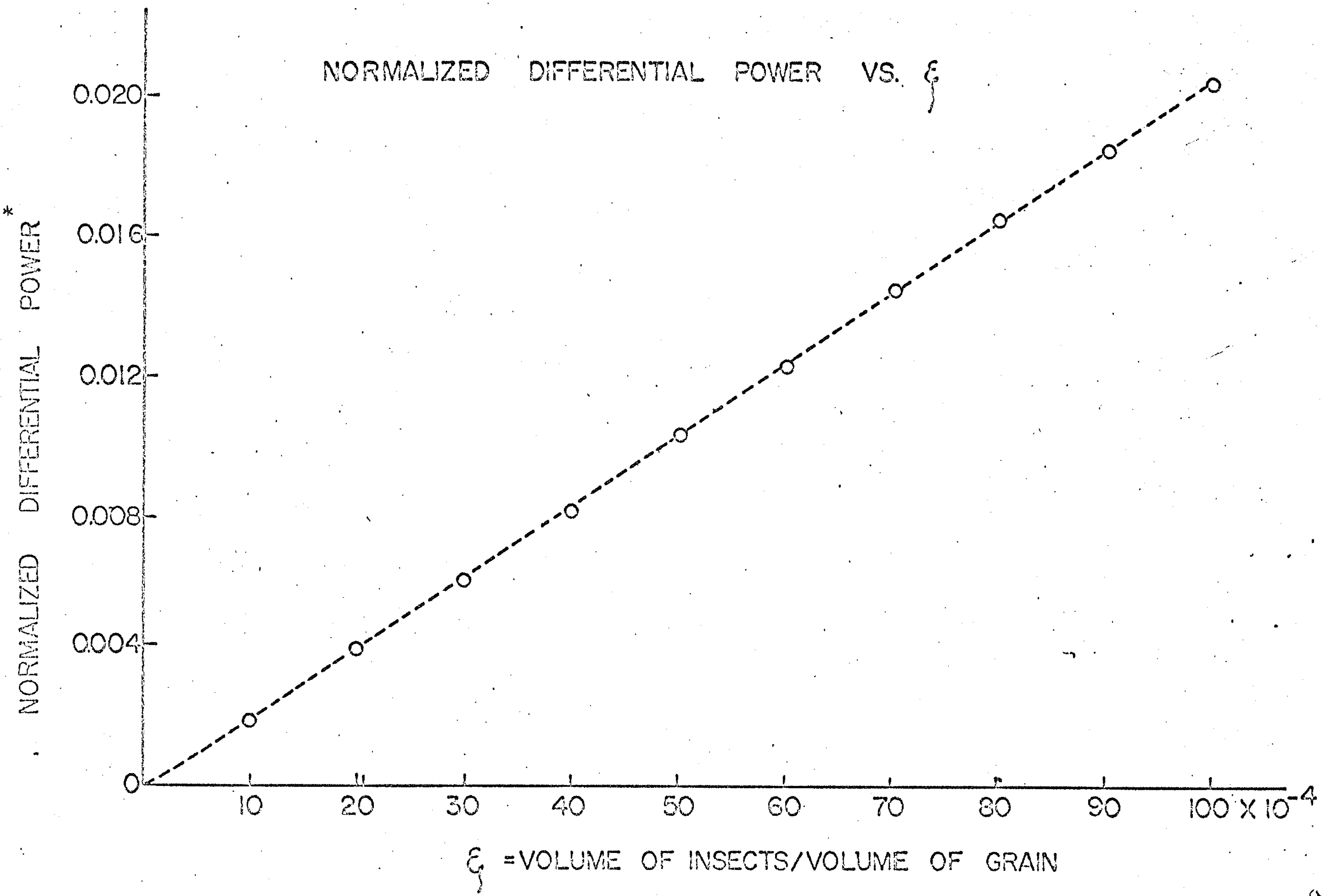

* Power loss in a lossy dielectric is directly proportional to ε'

$$R = \frac{-c}{2(\beta_1+c) - \frac{c^2}{2(\beta_1+c)\ldots\ldots}} \left(e^{-jzq} - e^{-j\ell q}\right) \tag{3.3.1}$$

where

$$c = k^2\chi/2\beta_1 \tag{3.3.2}$$

and

$$q = c - \frac{c^2}{2(\beta_1+c) - \frac{c^2}{2(\beta_1+c)\ldots}} \tag{3.3.3}$$

Equation (3.3.1) can be rewritten in the alternative form

$$R' = \left[\frac{\beta_1-\sqrt{\beta_1^2+k^2\chi}}{\beta_1+\sqrt{\beta_1^2+k^2\chi}} \right] \left(1 - e^{-j(\sqrt{\beta_1^2+k^2\chi} - \beta_1)\ell} \right) \tag{3.3.4}$$

where R' represents the reflection coefficient at z=0. The term between the square brackets in (3.3.4) represents the reflection coefficient for a semi-infinite slab. The results for R' vs ℓ based on (3.3.4) are plotted in figure (3.3.1).

3.4. MEASUREMENT OF SCATTERING COEFFICIENTS

Previous results for the scattering coefficients obtained with perturbation theory are compared with experimental measurement using Deschamp's graphical method. The experimental set up is shown in figure (3.4.1). The measurement procedure consists of placing a sliding short circuit at the output terminals of the grain sample and moving it through a series of points separated by 1/16 of a guided wavelength. The input impedances corresponding to each of the short circuit positions are measured and plotted on the reflection coefficient plane of the Smith chart resulting in a circle. If the radius of this circle is less than unity, then the sample is lossy, and

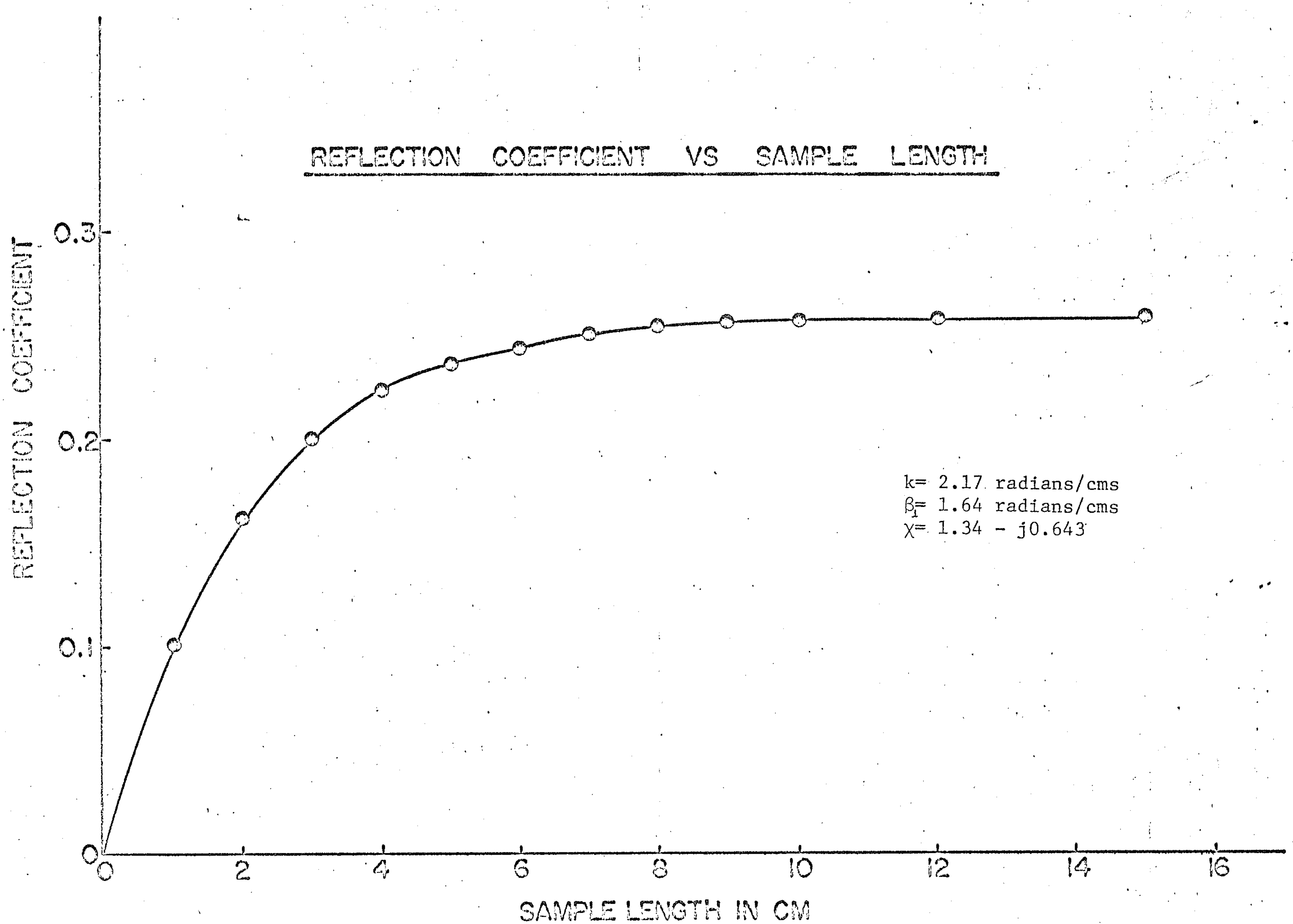
REFLECTION COEFFICIENT VS SAMPLE LENGTH
REFLECTION COEFFICIENT
0.3
0.2
0.1
0
0
2
4
6
8
10
12
14
16
SAMPLE LENGTH IN CM
k= 2.17 radians/cms
βi= 1.64 radians/cms
χ= 1.34 - j0.643

Fig. 3.3.1

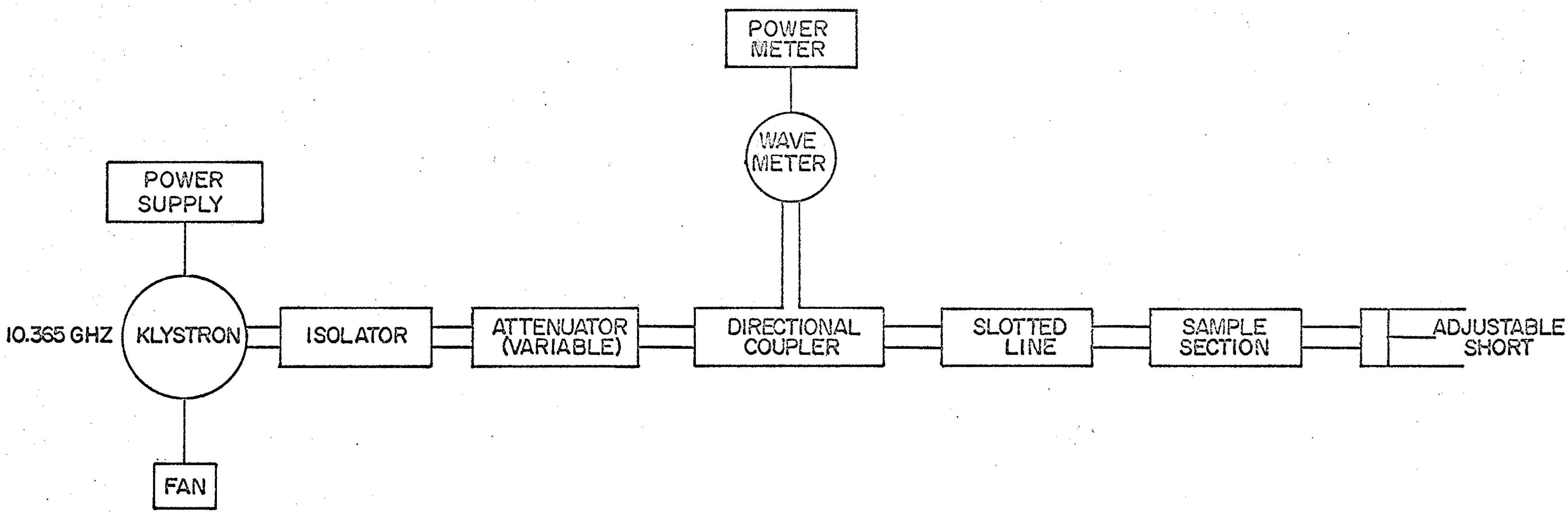

APPARATUS FOR MEASURING THE SCATTERING MATRIX COEFFICIENTS OF GRAIN AND FLOUR SAMPLES

Fig. 3.4.1

CONSTRUCTION OF THE DESCHAMPS CIRCLE FROM EXPERIMENTAL DATA

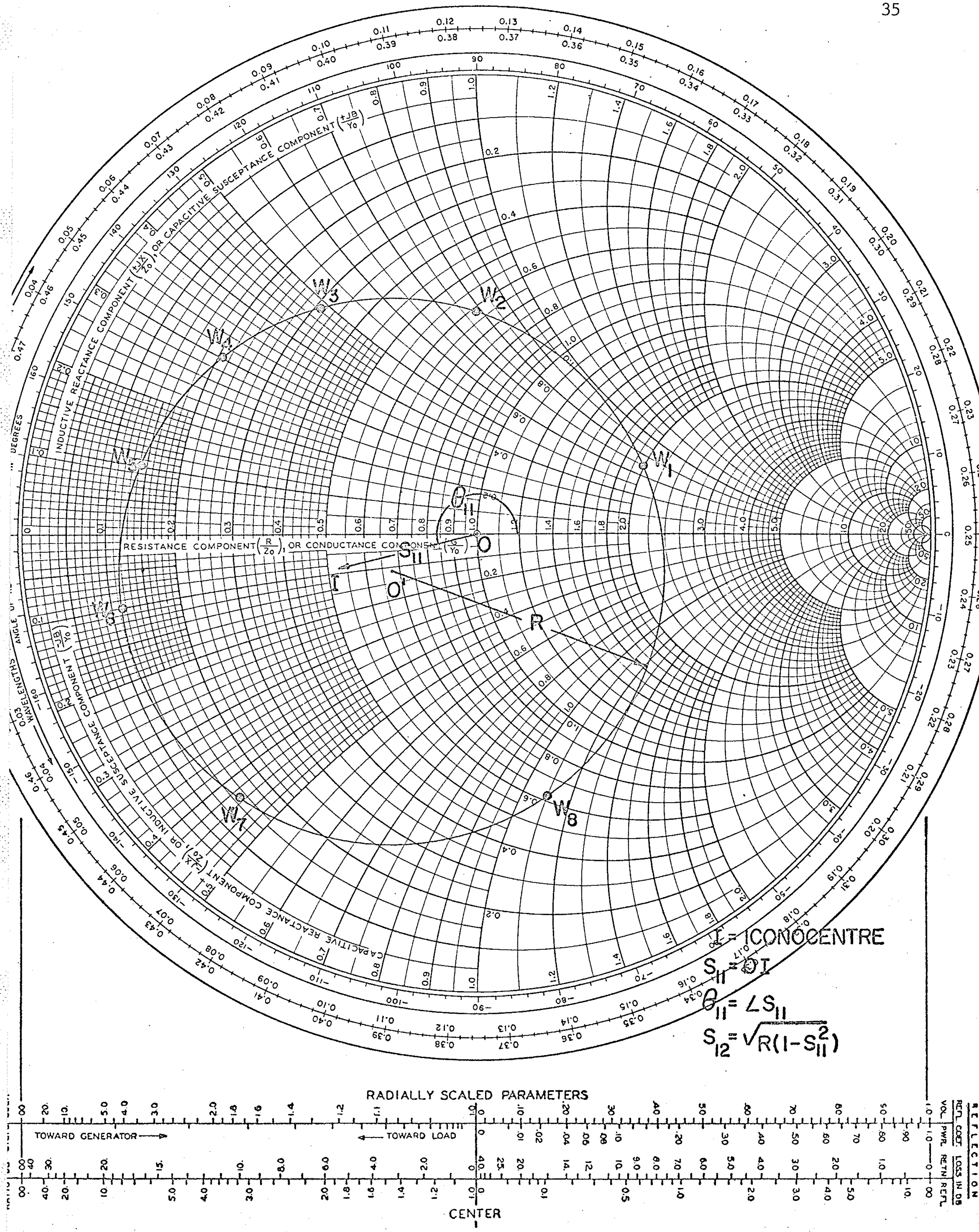

Fig. 3.4.2

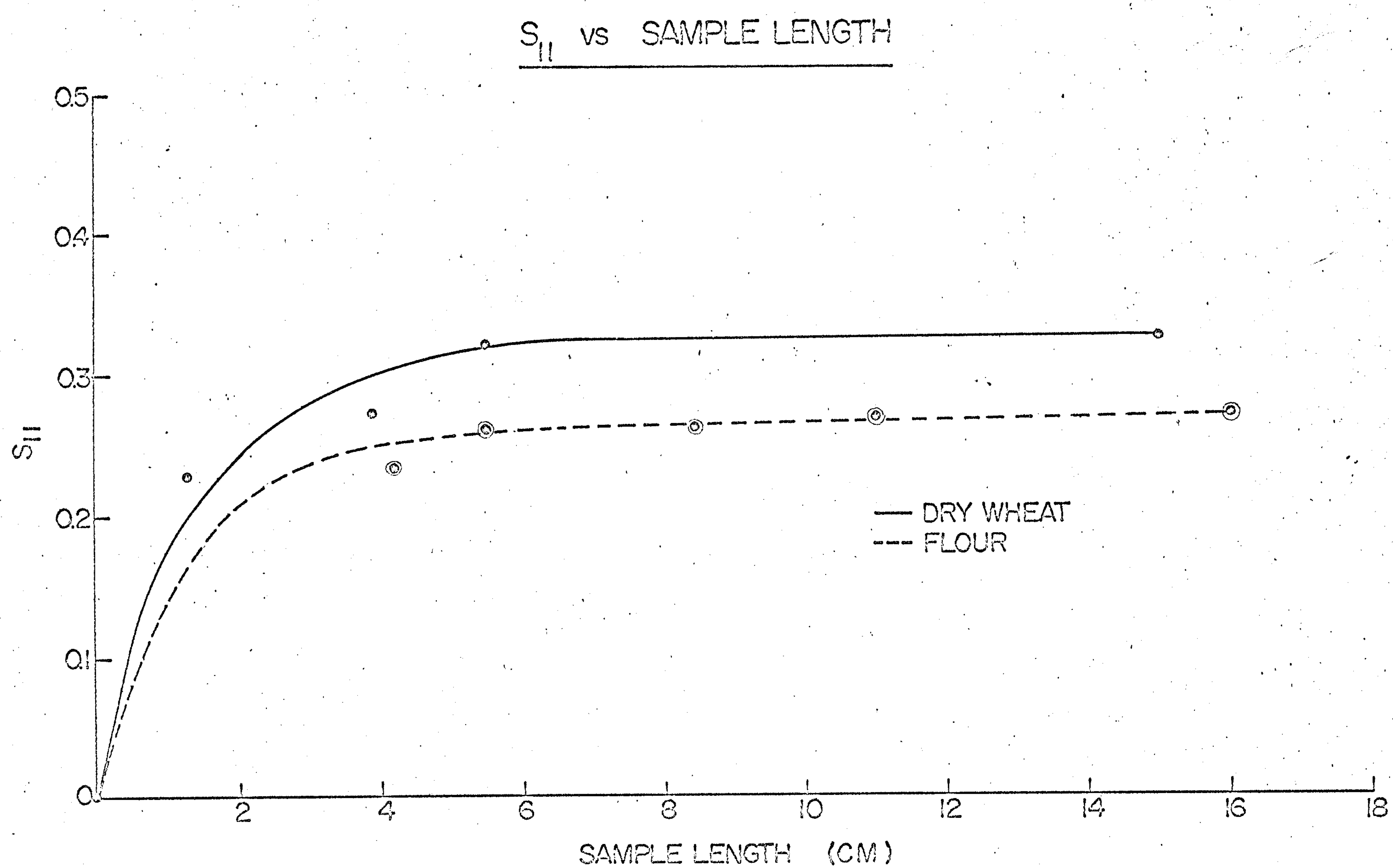

S11 VS SAMPLE LENGTH
0.5
0.4
0.3
0.2
0.1
0
S11
2
4
6
8
10
12
14
16
18
SAMPLE LENGTH (CM)
DRY WHEAT
FLOUR

Fig. 3.4.3.

if the radius is unity, the sample is lossless. The circle shown in figure (3.4.2) is for a test sample of 1.95 cms. The test was carried with a x-band equipment at frequency 10.365 GHZ. The procedure is repeated for different lengths of the sample and results of S_{11} vs ℓ are plotted in figure (3.4.3).

3.5 CONCLUSIONS

A method for calculating the equivalent dielectric constant of infested grain has been presented using Taylor's formula [24]. The insects have been assumed to be small spheres having a random distribution. This equivalent dielectric constant can be utilized to detect the concentration of insects in a particular volume of grain.

The results for the reflection coefficient are found to be in reasonable agreement with experiment. Although theoritical results were obtained for the detection of insects, no proper experimental verification could be made due to the small volume of the insects and inadequacy of the experimental set up used. However the detection may be possible for a larger volume of the insects.

One practical application of the theory is to calculate the necessary power to be dissipated in infested grain in order to design the apparatus required to kill the insects by microwave power. The success of such practical schemes has already been established [25] and is based on the selective heating of mixed dielectrics.

CHAPTER IV

DISCUSSION OF RESULTS AND CONCLUSIONS

4.1 GENERAL

A perturbation analysis which can be utilized for an axially dependent perturbation in an otherwise axially uniform structure has been developed. The technique is iterative and utilizes the expansion of fields in a complete set of unperturbed modes. Due to the provision of a nonlinear term in the correction to the phase progression function, it is possible to obtain directly the correction to the phase progression in the incident mode. Thus Richter's theory facilitates direct calculation of propagation constant and phase shift introduced by a dielectric perturbation, except for the limitations explained in the introduction.

Results have been presented here for the propagation constant and related parameters, for one or more E-plane or H-plane slabs with faces parallel to and at arbitrary distances from the waveguide walls. The solutions are obtained using a closed form expression for the contributions from the dominant scattered mode. The contributions from the next scattered mode are considered up to the third order. Contributions from still higher modes have been found to be negligible in most of the cases considered. The following example for the eleven slab case illustrates the magnitude of terms corresponding to various modes.

Perturbation parameter = $2G_{11}k^2/\beta_1^{\ 2}$ = 5.14

	k_z/β_1
Contribution from dominant scattered mode (p=-1) to all orders	2.4800
Contribution from next scattered mode (p=+3,-3) to second order	0.1820
Contribution from next scattered mode (p=+3,-3) to third order	-0.1077
	2.5543

$k_z/k_o = (k_z/\beta_1)(\beta_1/k_o) = 1.836$, error [26] = 3.96%

There are two main advantages in using this procedure.

1) Results can be obtained even when the magnitude of the perturbation parameter ($2G_{11}k^2\chi/\beta_1^2$ or $2G_{11}k^2/\beta_1^2$) is more than unity.

2) Results with reasonable accuracy can be obtained even for the most difficult case of structures where the propagation constant has to be perturbed from a real to an imaginary value, which is a rather complicated problem. Some extreme cases of this nature have been considered (2.3.1a and 2.3.1d). However the results presented are reasonable when one considers the fact that, along with the above difficulty, the condition for the convergence of the perturbation series also does not hold in most of the cases studied.

4.2 COMPARISON WITH EXACT OR EXPERIMENTAL RESULTS

The results obtained for the propagation constant and cut off wavelength have been compared with exact solutions obtained by transverse resonance techniques and numerical solution of transcendental equations [1-5 ,21,23]. Since exact results for a finite dielectric slab are not available, we have compared our results with experiment.

The agreement with the experiment and the exact solution is good. The maximum error in most cases is around 7%. The error is found to increase to 10-15% in extreme cases where we either deal with very high dielectric constant (ε=16) or when the propagation constant is perturbed from a real to an imaginary value, or both.

4.3 CONCLUSIONS

In conclusion therefore we have shown that reasonably accurate results may be obtained for E or H-plane dielectric slab perturbations even when the perturbation parameter is allowed to exceed unity and the propagation constant is perturbed from real to an imaginary value. These advantages have been amply demonstrated and permit the application of Richter's theory to many cases where it was predicted to fail.

4.4. SUGGESTIONS FOR FUTURE RESEARCH

There is an unlimited scope for research in the field of inhomogeneously filled dielectric waveguides. An obvious extension is the case of four different slabs filling the cross-section of a waveguide as shown in figure (4.1a). The author has attempted a first order solution for the specific case of $\varepsilon_1=\varepsilon_4=3.5$ and $\varepsilon_2=\varepsilon_3=3.75$. However the experimental results have been found to be significantly different from the theoretical results. These first order results could still be useful for very low dielectric constants.

An attempt should also be made to extend the theory to a randomly filled cross-section. Some work has been done on this subject. Richter [1-3] has given 4 x 4 perturbation matrix for the problem but nothing further has been done. Holmes [27] has attempted to use the Wentzel, Kramers and Brillouin (WKB) approximation. This method however depends upon the asymptotic formulas or on slow variation of perturbations within a wavelength. Karbowiak [28] has tried to solve the problem from a transmission line viewpoint by constructing an equivalent circuit of n-coupled transmission lines. The random characteristics of the perturbation have been taken into account by assuming an equivalent random coupling between the modes of the homogeneous system. However no mention has been made of the choice of coupling coefficients for a specific perturbation. The theory presented here can be utilized to calculate the results only up to the first order. Higher order terms are difficult to compute because

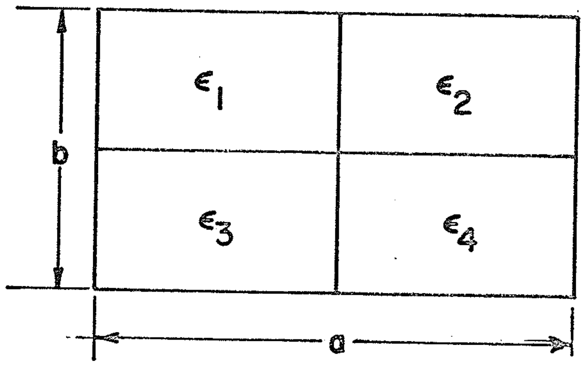

a) WAVEGUIDE LOADED WITH DIFFERENT DIELECTRICS

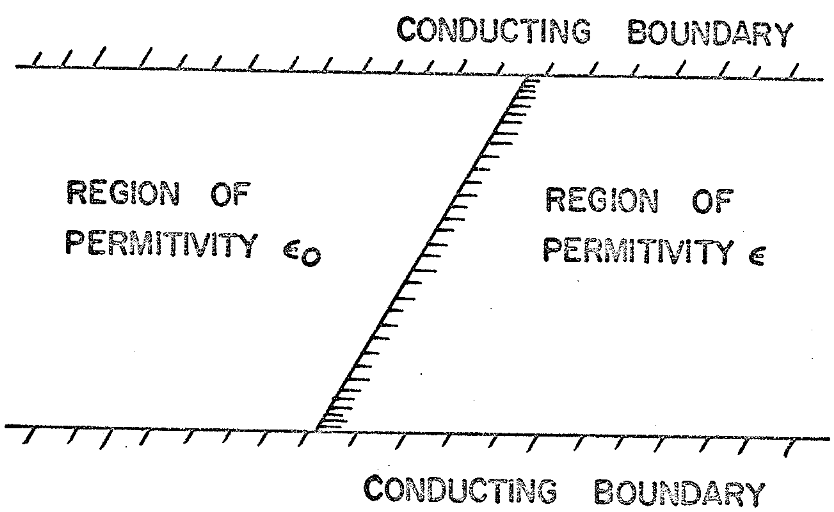

b) H-PLANE WEDGE

FUTURE RESEARCH PROBLEMS

Fig. 4.1

they involve coupling between various types of scattered modes.

Further research should be done to utilize the fact that the theory is particularly useful for problems involving axially dependent perturbations. The case of an H-plane wedge as shown in figure (4.1b) is an example of such a problem. Ray Optical solutions have been attempted for this problem [29] but with insufficient confidence because of the difficulty of summing the contributions from the diffracted rays.

Finally the application of the theory is suggested to the case of a ferrite or plasma loaded waveguide. The perturbation matrix should be capable of taking into account the tensor nature of the perturbation. Some perturbational and variational methods [5,7] for the former case have been proposed for very small perturbations.

Further extension of the work presented in this thesis may lead to reasonable results in all these cases where the exact solutions are not available or are too complicated.

BIBLIOGRAPHY

[1] Hord, W.E.,and Rosenbaum, F.J.,"Approximation Technique for Dielectric Loaded Waveguides", I.E.E.E. Transactions on Microwave Theory and Techniques, Vol. MTT-16,No.4,pp.228-233, April 1968.

[2] Vertanian, P.H., Ayres,W.P., and Helgesson, A.L., "Propagation in Dielectric Loaded Rectangular Waveguides", I.R.E. Transactions on Microwave Theory and Techniques, Vol. MTT-6,pp. 215-222, April 1958.

[3] Eberhardt, N., " Propagation in the Off Centre E-plane Dielectrically Loaded Waveguide", I.E.E.E. Transactions on Micrwave Theory and Techniques, Vol. MTT-15, pp. 282-289, May 1967.

[4] Davies, J.B., "Propagation in Rectangular Waveguides Filled with Uniaxial Dielectric", I.E.E.E. Transactions on Microwave Theory and Techniques, Vol. MTT-15, pp. 372-376, June 1967.

[5] Button, K.J., and Lax, B., "Perturbation Theory of the Reciprocal Ferrite Phase Shifter", Proceedings I.E.E. (London), Vol. 109B, Suppl. 21 pp. 56-58, 1962.

[6] Bland, G.F., and Franco, A.G., "Phase Shift Characteristics of Dielectric Loaded Waveguide" I.R.E. Transactions on Microwave Theory and Techniques, Vol. MTT-10, pp. 492-496, November 1962.

[7] Soohoo, R.F., "Theory of Dielectric Loaded and Tapered Field Ferrite Devices", I.R.E. Transactions on Microwave Theory and Techniques, Vol. MTT-9, pp. 220-224, May 1961.

[8] Harrington, R.F., "Time Harmonic Electromagnetic Fields", New York, McGraw-Hill, 1961, pp. 152-163.

[9] Collin, R.E., "Field Theory of Guided Waves", New York, McGraw-Hill, 1961, pp. 224-229.

[10] Berk, A.D., "Variational Principles for Electromagnetic Resonators and Waveguides", I.R.E. Transactions on Antennas and Propagation, Vol. AP-4, pp. 104-111, April 1956.

[11] Richter, S.L., Diament, P., and Schlesinger, S.P.,"Perturbation Analysis of Axially Nonuniform Structures using Nonlinear Phase Progression", I.E.E.E. Transactions on Antennas and Propagation, Vol. AP-15, No. 3, pp. 422-430, May 1967.

[12] Richter, S.L., Diament, P., and Schlesinger, S.P.,"Electromagnetic Propagating Structurec with Nonuniform Gross Perturbations, I.E.E.E. Transactions on Antennas and Propagation, Vol. AP-15, No. 3, pp. 431-436, May 1967.

[13] Richter, S.L.,"Guided Waves in Bounded Media with Random Gross Inhomogeneties", I.E.E.E. Transactions on Antennas and Propagation, Vol. AP-15, No. 1, pp. 70-75, January 1967.

[14] Richter, S.L., Diament, P., and Schlesinger, S.P.,"Axially Dependent Perturbation Analysis using Nonlinear Phase Progression', Department of Electrical Engineering, Columbia University, New York, Scientific Rept. 89, May 1966.

[15] Dirac, P.A.M.,"On the Theory of Quantum Mechanics", Proceedings Royal Society (London), Vol. A112, pp. 661-667, 1926.

[16] Schroedinger, E.,"Quantisierung als Eigenwert Problem", Ann Der Phys. Vol. 80, No. 13, pp. 437-490, 1926.

[17] Gabrial, G.J., and Brodwin, M.E.,"The Solution of Guided Waves in Inhomogeneous Anisotropic Media by Perturbational and Variational Methods", I.E.E.E. Transactions on Microwave Theory and Techniques,

[18] Leonard-Jones. J.E."Perturbation Problem in Quantum Mechanics", Proc. Royal Soc. (London), Vol. A129, pp. 598-615, 1930.

[19] Brillouin, L.,"Problems of Perturbations and Self-consistant Fields", J. Physics Radium, Vol. 3, pp. 373-389, September 1932.

[20] Morse, P.M., and Feshbach, H.,"Methods of Theoretical Physics", New York, McGraw-Hill, 1953.

[21] Ellerbruch, D.A.,"U.H.F. and Microwave Phase Shift Measurements", Proceedings of I.E.E.E.,,Vol. 55, No. 6, pp. 960-969, June 1967.

[22] Dyson, J.D.,"Measurement of Phase at U.H.F. and Microwave Frequencies", I.E.E.E. Transactions on Microwave Theory and Techniques, Vol. MTT-14, No. 9, pp. 410-423, September 1966.

[23] Marcuvitz, N.,"Waveguide Handbook", McGraw-Hill, 1951, pp. 387-393.

[24] Taylor, L.S.,"Dielectric Properties of Mixtures", I.E.E.E. Transactions on Antennas and Propagation,Vol. AP-13, No. 6,pp. 943-947, November 1965.

[25] Hamid, M.A., Kashyap, S.C. and Van Cauwenberghe, R., "Control of Grain Insects by Microwave Power", The Journal of Microwave Power, vol.3, no.3, September 1968.

[26] Wexler, A., "Rectangular Waveguides Loaded with an Arbitrary Number of Slabs", Private Communication.

[27] Holmes, D.A., "Propagation in Rectangular Waveguide Containing Inhomogeneous, Anisotropic Dielectric", I.E.E.E. Transactions on Microwave Theory and Techniques, vol.MTT-12, no.3, pp. 152-155, March 1964.

[28] Karbowiak, A.E., "Guided Waves in Statistically Random Media", Proceedings of the I.E.E., vol.3, no.2, pp. 222-230, February 1964.

[29] Robinson, J.E., "Ray Propagation in Dielectric Loaded Waveguides", M.Sc. Thesis, University of Manitoba, July 1967.

APPENDIX A2.1

DERIVATION OF (2.3.1)

Maxwell's equations for the TE_{no} case can be reduced to the form

$$\partial E_y/\partial z = +j\omega\mu_o H_x \qquad (A2.1.1)$$

$$\partial E_y/\partial x = -j\omega\mu_o H_z \qquad (A2.1.2)$$

$$\partial H_x/\partial z - \partial H_z/\partial x = j\omega\varepsilon_o \varepsilon E_y \qquad (A2.1.3)$$

From (A2.1.1) to (A2.1.3) we have

$$\partial E_y/\partial z = j\omega\mu_o H_x \qquad (A2.1.4)$$

$$\partial H_x/\partial z = -\frac{1}{j\omega\mu_o}\frac{\partial^2 E_y}{\partial x^2} + j\omega\varepsilon_o \varepsilon E_y \qquad (A2.1.5)$$

(A2.1.4) and (A2.1.5) can be put in the matrix form

$$\begin{bmatrix} o & j\omega\mu_o \\ -\frac{1}{j\omega\mu_o}\frac{\partial^2}{\partial x^2} + j\omega\varepsilon_o & o \end{bmatrix} \begin{bmatrix} E_y \\ H_x \end{bmatrix} + \begin{bmatrix} o & o \\ j\omega\varepsilon_o(\varepsilon-1) & o \end{bmatrix} \begin{bmatrix} E_y \\ H_x \end{bmatrix} = \frac{\partial}{\partial z}\begin{bmatrix} E_y \\ H_x \end{bmatrix} \qquad (A2.1.6)$$

APPENDIX A2.2

DERIVATION OF (2.3.33)

Equations (2.3.18) to (2.3.23) can be used to get the expressions for f_o and u_p for various orders of perturbation.

from (2.3.18)

$$f_o^{(1)} = k^2\chi G_{11} z/\beta_1 \;, \quad G_{pq} = \frac{1}{a}\int_{x_1}^{x_2} \sin(p\pi x/a)\sin(q\pi x/a)\; dx \qquad \text{(A2.2.1)}$$

from (2.3.22)

$$\partial u_p^{(1)}/\partial z = k^2\chi G_{p1} e^{-j(\beta_1-\beta_p)z} \;/\; j\beta_1 \qquad \text{(A2.2.2)}$$

$$u_p^{(1)} = \frac{k^2\, G_{p1}\chi}{\beta_1(\beta_1-\beta_p)}\, e^{-j(\beta_1-\beta_p)z} \qquad \text{(A2.2.3)}$$

from (2.3.19) and (A2.2.3)

$$\partial f_o^{(2)}/\partial z = \sum_p \left(k^4\chi^2 G_{p1}^2\right)/\left(\beta_1\beta_p(\beta_1-\beta_p)\right) \qquad \text{(A2.2.4)}$$

$$f_o^{(2)} = \sum_p \frac{k^4\chi^2 G_{p1}^2\; z}{\beta_1\beta_p(\beta_1-\beta_p)} \qquad \text{(A2.2.5)}$$

from (2.3.23), (A2.2.1) and (A2.2.3)

$$\partial u_p^{(2)}/\partial z = k^4\chi^2 G_{p1} G_{pp} e^{-j(\beta_1-\beta_p)z}/\left(j\beta_1\beta_p(\beta_1-\beta_p)\right)$$
$$- \; k^4\chi^2 G_{p1} G_{pp} e^{-j(\beta_1-\beta_p)z}/\beta_1^{\,2} \qquad \text{(A2.2.6)}$$

$$u_p^{(2)} = \frac{K^4\chi^2 G_{11}}{\beta_1(\beta_1-\beta_p)}\, e^{-j(\beta_1-\beta_p)z}\left[\frac{G_{pp}}{\beta_p(\beta_1-\beta_p)} - \frac{G_{11}}{\beta_1}\, z - \frac{G_{11}}{\beta_1(\beta_1-\beta_p)}\right] \qquad \text{(A2.2.7)}$$

from (2.3.22) and (A2.2.7)

$$\partial f_o^{(3)}/\partial z = \sum_p jk^6\chi^3 G_{p1}^2 G_{11}/(\beta_1{}^2\beta_p(\beta_1-\beta_p))$$

$$+ \sum_p k^2\chi G_{p1} u_p^{(2)} e^{-j(\beta_1-\beta_p)}/\beta_1 \qquad \text{(A2.2.8)}$$

$$f_o{}^{(3)} = \sum_p \frac{k^6\ \chi G_{p1}^2 z}{\beta_1\beta_p(\beta_1-\beta_p)^2}\left[\frac{G_{pp}}{\beta_p} - \frac{G_{11}}{\beta_1}\right] \qquad \text{(A2.2.9)}$$

and so on for higher orders.

APPENDIX A2.3

DERIVATION OF (2.4.1) TO (2.4.7)

Equations (2.3.18) to (2.3.23) can be used to get the expressions for $\bar{f}_o$ and u_p for a finite dielectric perturbation.

From (2.3.18)

$$f_o^{(1)} = k^2 \chi G_{11} z/\beta_1 \qquad o<z<\ell \qquad \text{(A2.3.1)}$$

From (2.3.22)

$$\partial u_p^{(1)}/\partial z = k^2 \chi G_{p1} e^{-j(\beta_1-\beta_p)z}/j\beta_1 \qquad \text{(A2.3.2)}$$

Integrating

$$u_p^{(1)} = \frac{k^2\chi}{\beta_1} G_{p1}(x_1,x_2)h(z)\frac{e^{-j(\beta_1-\beta_p)\min(z,\ell)}-1}{\beta_1-\beta_p} \qquad p>1 \qquad \text{(A2.3.3)}$$

$$= \frac{k^2\chi}{\beta_1} G_{p1}(x_1,x_2)h(\ell-z)\ \frac{e^{-j(\beta_1-\beta_p)z h(z)}-e^{-j(\beta_1-\beta_p)\ell}}{(\beta_1-\beta_p)} \qquad p<o \qquad \text{(A2.3.4)}$$

From (2.3.19) and (A2.3.3)

$$\partial f_o^{(2)}/\partial z = k^4\chi^2 G_{p1}^2 (\ 1 - e^{-j(\beta_1-\beta_p)(\ell- z)})/(\beta_1\beta_p(\beta_1-\beta_p)) \quad p<o \qquad \text{(A2.3.5)}$$

From (2.3.19) and (A2.3.4)

$$\partial f_o^{(2)}/\partial z = k^4\chi^2 G_{p1}^2 (1 - e^{j(\beta_1-\beta_p)z}/(\beta_1\beta_p(\beta_1-\beta_p)) \qquad p>1 \qquad \text{(A2.3.6)}$$

$$f_o^{(2)} = \sum_p \frac{k^4\chi^2 G_{p1}^2}{\beta_1\beta_p(\beta_1-\beta_p)} \left[z + \frac{2j}{\beta_1-\beta_p} \cos\{(\beta_1-\beta_p)z/2\}\ e^{-j(\beta_1-\beta_p)(\ell-z/2)} \right], \ p<0 \qquad \text{(A2.3.7)}$$

$$= \sum_p \frac{k^4\chi^2 G_{p1}^2}{\beta_1\beta_p(\beta_1-\beta_p)} \left[z + \frac{j}{\beta_1-\beta_p} \ \{ e^{j(\beta_1-\beta_p)z} - 1 \} \right], \ p>1 \qquad \text{(A2.3.8)}$$

From (2.3.23), (A2.3.1) and (A2.3.3)

$$\partial u_p^{(2)}/\partial z = k^4\chi^2 G_{p1} G_{pp} (e^{-j(\beta_1-\beta_p)z} - e^{-j(\beta_1-\beta_p)\ell}\}/(j\beta_1\beta_p(\beta_1-\beta_p))$$

$$- k^4\chi^2 G_{p1}G_{11} z\, e^{-j(\beta_1-\beta_p)z}/\beta_1^2 \qquad p<o \qquad \text{(A2.3.9)}$$

Integrating

$$u_p^{(2)} = \frac{k^4\chi^2 G_{p1}}{\beta_1(\beta_1-\beta_p)} \left[\frac{G_{pp}}{\beta_p(\beta_1-\beta_p)} \{ e^{-j(\beta_1-\beta_p)z} - e^{-j(\beta_1-\beta_p)\ell} \} + \right.$$

$$\frac{j\,G_{pp}}{\beta_p} e^{-j(\beta_1-\beta_p)\ell}(z-\ell) - \frac{j\,G_{11}}{\beta_1}(ze^{-j(\beta_1-\beta_p)z} - \ell e^{-j(\beta_1-\beta_p)\ell})$$

$$\left. \frac{G_{11}}{\beta_1(\beta_1-\beta_p)} (e^{-j(\beta_1-\beta_p)z} - e^{-j(\beta_1-\beta_p)\ell}) \right], \; p<0 \qquad \text{(A2.3.10)}$$

From (2.3.23), (A2.3.1) and (A2.3.4)

$$\delta u_p^{(2)}/\delta z = k^4\chi^2 G_{pp}G_{p1}(e^{-j(\beta_1-\beta_p)z} - 1)/(j\beta_1\beta_p(\beta_1-\beta_p))$$

$$- k^4\chi^2 G_{p1}G_{11} z\, e^{-j(\beta_1-\beta_p)z}/\beta_1^2 \qquad p>1 \qquad \text{(A2.3.11)}$$

$$u_p^{(2)} = \frac{k^4\chi^2 G_{p1}}{\beta_1(\beta_1-\beta_p)} \left[\frac{G_{pp}}{\beta_p(\beta_1-\beta_p)} (e^{-j(\beta_1-\beta_p)z} - 1) + \frac{jG_{pp}z}{\beta_p} \right.$$

$$\left. - \frac{jG_{11}z}{\beta_1} e^{-j(\beta_1-\beta_p)z} - \frac{G_{11}}{\beta_1(\beta_1-\beta_p)} (e^{-j(\beta_1-\beta_p)z} - 1) \right], \; p>1 \qquad \text{(A2.3.12)}$$

APPENDIX A2.4.

DERIVATION OF (2.6.4) AND (2.6.5)

Maxwell's equations for TM to y case reduce to the form

$$\delta E_z/\delta y - \delta E_y/\delta z = -j\omega\mu_o H_x \tag{A2.4.1}$$

$$\delta E_y/\delta x - \delta E_x/\delta y = -j\omega\mu_o H_z \tag{A2.4.2}$$

$$\delta H_x/\delta z - \delta H_z/\delta x = j\omega\varepsilon_o \varepsilon E_y \tag{A2.4.3}$$

$$-\delta H_x/\delta y = j\omega\varepsilon_o \varepsilon E_z \tag{A2.4.4}$$

Use of (A2.4.1) to (A2.4.4) and other relations for TM to y modes [13] we have

$$\delta E_y/\delta z = j\omega\mu_o H_x - (\delta^2 H_x/\delta y^2)/(j\omega\varepsilon_o) \tag{A2.4.5}$$

$$\delta H_x/\delta z = j\omega\varepsilon E_y - (k^2\delta^2 E_y/\delta x^2)/(j\omega\mu_o)(k^2 - n^2\pi^2/b^2) \tag{A2.4.6}$$

(A2.4.5) and (A2.4.6) can be put in the following matrix form

$$\begin{bmatrix} o & \frac{-1}{j\omega\varepsilon_o}(1/\varepsilon-1)\frac{\partial^2}{\partial y^2} \\ -j\omega\varepsilon_o(\varepsilon-1) & o \end{bmatrix} \begin{bmatrix} E_y \\ H_x \end{bmatrix}$$

$$\begin{bmatrix} o & \frac{-1}{j\omega\varepsilon_o}\frac{\partial^2}{\partial y^2} + j\omega\mu_o \\ \frac{1}{j\omega\mu_o}\frac{k^2}{k^2-(n\pi/b)^2}\frac{\partial^2}{\partial x^2} + j\omega\varepsilon_o & o \end{bmatrix} \begin{bmatrix} E_y \\ H_x \end{bmatrix} = \frac{\delta}{\delta z}\begin{bmatrix} E_y \\ H_x \end{bmatrix}$$

(A2.4.7)